Challenges and issues in continuum modelling of tribology, wear, cutting and other processes involving high-strain rate plastic deformation of metals

Amir Mir[a], Xichun Luo[b], Iñigo Llavori[c], Anish Roy[d], Danka Labus Zlatanovic[e,f], Shrikrishna N. Joshi[g] and Saurav Goel[a,g,h*]

[a]School of Engineering, London South Bank University, 103 Borough Road, London, SE1 0AA, UK

[b]Centre for Precision Manufacturing, Department of Design, Manufacture and Engineering Management, University of Strathclyde, Glasgow, UK

[c]Mechanical and Industrial Manufacturing Department, Mondragon Unibertsitatea, Loramendi 4, 20500, Mondragón, Spain

[d]Wolfson School of Mechanical, Electrical and Manufacturing Engineering, Loughborough University, Loughborough, Leicestershire LE11 3TU, UK

[e]Department of Production Technology, Technische Universität Ilmenau, 98693 Ilmenau, Germany

[f]Department of Production Engineering, Faculty of Technical Science, University of Novi Sad, 21000 Novi Sad, Serbia

[g]Department of Mechanical Engineering, Indian Institute of Technology Guwahati, Guwahati, 781039, India

[h]University of Petroleum and Energy Studies, Dehradun, 248007, India

*Email: GoeLs@Lsbu.ac.uk

Abstract

Contribution of finite element method (FEM) as a modelling and simulation technique to represent complex tribological processes has improved our understanding about various biomaterials. This paper presents a review of the advances in the domain of finite element (FE) modelling for simulating tribology, wear, cutting and other processes involving high-strain rate plastic deformation of metals used in bio tribology and machining. Although the study is largely focused on material removal cases in metals, the modelling strategies can be applied to a wide range of

1

other materials. This study discusses the development of friction models, meshing and remeshing strategies, and constitutive material models. The mesh-based and meshless formulations employed for bio tribological simulations with their advantages and limitations are also discussed. The output solution variables including scratch forces, local temperature, residual stresses are analyzed as a function of input variables.

Keywords: Finite element, Lagrangian, ALE, meshless, chip formation

Nomenclature and Abbreviations:

σ_n=normal stress

σ_f=tensile failure stress

$\bar{\sigma}$=effective stress

σ^m=maximum stress

$\sigma_1, \sigma_2, \sigma_3$=principle stress

σ_y= yield stress

τ=shear stress

τ_{fl}=shear failure stress

τ_f=frictional shear stress

τ_c=limiting shear stress

$\bar{\varepsilon}$=effective strain

$\bar{\varepsilon}^p$=equivalent plastic strain

$\bar{\varepsilon}_f^p$=equivalent strain at failure

A,B,C,m,n=Johnson-Cook model parameters

d_1 to d_5=Johnson-Cook failure parameters

C_0 to C_5=Zerilli-Armstrong model parameters

F,L=Usui's wear model constants

σ^*=pressure to vonmises stress ratio ($\frac{p}{q}$)

$\dot{\varepsilon}_0$=reference strain rate

$\dot{\varepsilon}^p$=plastic strain rate

χ=thermal conductivity in temperature equation

$\dot{Q}$=rate of heat flux

C_p=specific heat

q=vonmises stress

m=shear friction factor (shear model)

k=shear flow stress (shear model)

F_c=tangential cutting force

F_t=thrust force

μ=coefficient of friction

μ_{adh}=adhesive friction coefficient

T_{mt}=melting temperature

T_{rm}=Room temperature

T_{mod}=velocity modified temperature

μ_{adh}=adhesive friction coefficient

k=shear flow stress

τ_c=limiting shear flow stress

R=Universal gas constant

ε^p=plastic strain

G(v,f) =Takeyama-Morata abrasive wear term

PSZ = primary shear zone

SDZ = Secondary deformation zone

TDZ = Tertiary deformation zone

SPH = Smoothed particle hydrodynamics

LAG= Lagrangian

EUL=Eulerian

2

ALE= Arbitrary Lagrangian Eulerian

PFEM= Particle finite element method

EFG= Element Free Gelarkin

JC= Johnson-Cook

DEM= Discrete element method

C-L= Cockroft-Latham

FPM= Finite Pointset method

T-M= Takeyama and Murata

v=strain rate sensitivity constant

h_c=heat transfer coefficient

ϕ_s=shear plane angle

L_S = sliding region

L_t = sticking region

C_i=Cockroft-Latham damage parameter

P= hydrostatic pressure

q_f=frictional heat

V_r=tool-chip relative velocity

V_{ls}=average local sliding velocity

1. Introduction

Machining is a complex phenomenon which is known to depend on the friction between the cutting tool and the workpiece, cutting temperature, adiabatic shearing, stresses, strains, and strain rate. The literature reported in the past suggests the use of simulations, particularly, the finite element method to understand the convoluted phenomenon of machining mechanism in a simple and cost-effective manner. These models can be expressively classified based on analytical, experimental, numerical, and empirical as well as hybrid types [1, 2]. The development of machining techniques starting from conventional to the ultra-precision micro/nanoscale is highly dependent on these predictive models.

Using FEA, the qualitative and quantitative analyses of cutting process are conducted to obtain detailed analysis of chip morphologies, cutting forces, temperature, stresses and strains, and other output variables. Machining simulations analogous to any other simulations adopt input parameters that define the implicit

3

functional relationship in the explicit form of output variables. The FE machining studies are based on a variety of analyses including tool geometry [3-8], machining parameters and conditions (cryogenic, laser/water jet-assisted, etc.) [9-16], workpiece orientation [17, 18], tool wear measurement [5, 19, 20], chip separation criteria [21-25] and meshing and remeshing techniques [26-29]. The constitutive material models with different numbers and range of parameters were evaluated for a wide range of materials. Evaluation of input parameters using experimental studies in combination with numerical studies provides an improved understanding of machining mechanics of materials [30, 31]. Fig. 1 shows a list of input variables evaluated under experimental and simulated conditions for the required output solution variables.

A comprehensive bibliography of finite element (FE) simulations of various machining work from 1976-1996 can be found from Mackerle [32]. The pioneering studies of the cutting simulation were mainly focused on two-dimensional orthogonal models. The FE simulations of three-dimensional models increased with the development of high computational power and robust solvers [33] as well as strategies to reduce the computational cost [34, 35].

```
┌─────────────────────────────┐        ┌─────────────────────────────┐
│       Input variables       │        │       Input variables       │
│ (speed, feed, depth of cut, │        │ (speed, feed, depth of cut, │
│   tool geometry, machining  │        │  friction criteria, tool    │
│        conditions)          │        │  wear criteria, material    │
│                             │        │        models)              │
└─────────────────────────────┘        └─────────────────────────────┘
              │                                      │
              ▼                                      ▼
      ┌───────────────┐                      ┌───────────────┐
      │  Experimental │                      │   FE Cutting  │
      │  Cutting test │                      │   Simulation  │
      └───────────────┘                      └───────────────┘
```

Online measurement   Offline measurement   Direct calculations   Indirect calculation

| Cutting forces, temperature, chip formation | Chip geometry, tool wear, phase transformation, surface profile, tool-chip contact length | Chip geometry, cutting forces, stresses, strain, temperature, hydrostatic pressure | Tool wear, phase transformation, surface profile |

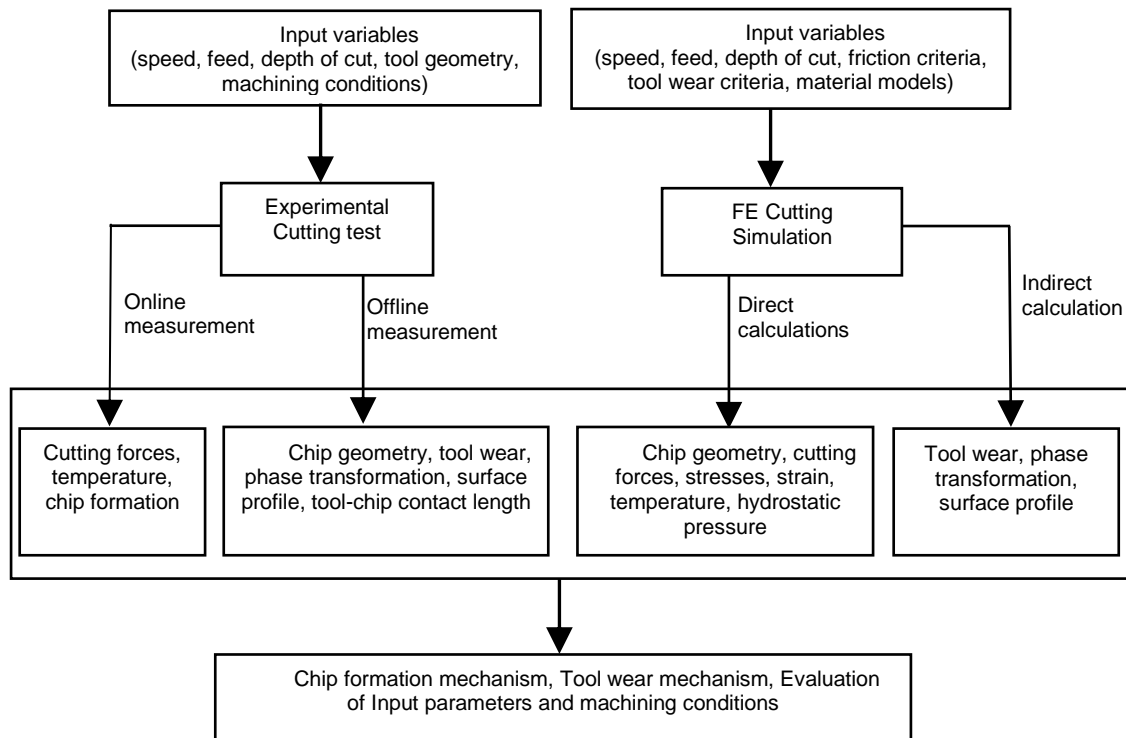Chip formation mechanism, Tool wear mechanism, Evaluation of Input parameters and machining conditions

Fig.1: Experimental and FE cutting simulation input and output variables

Although finite element simulations of machining processes involve simulations of turning [21], drilling [36, 37], milling [38-42], grinding [43, 44] along with other machining processes [32, 45-47], this paper deals with an investigation of basic cutting methodology with wedge shape tool adopted in these machining operations. The review is mainly based on machining simulation of metals of ductile, hard and brittle nature. There are many metals including Cr, Co and Ni as well as ceramics such as alumina and zirconia which are considered ideal for implants and dentistry applications. In orthopaedic surgery procedures, various machining procedures are involved including drilling, milling, sawing etc. Since human bone is of semi-brittle nature, its material removal behaviour can be effectively studied using different FEM techniques using robust material models [48, 49]. In the following sections, the development of FEM for the cutting process from the perspective of commercial software, FEM formulations, chip separation criteria, tool wear modelling, material

constitutive models, friction models, and meshing and remeshing techniques are discussed.

2. Finite element software for machining

The use of FEM for machining simulations started in the early 1970s when user-defined FE codes emerged. Later with the development of commercial software, machining studies were performed using general-purpose FE codes including NIKE 2D [45, 50-52], Abaqus [8, 26, 53-56], LS-DYNA [57, 58], ANSYS [59] and Marc [45, 60, 61]. These softwares have the capability to perform mechanical, thermal and coupled thermo-mechanical analysis. In recent years, researchers started using specialized metal cutting simulation software AdvantEdge [30, 41, 45, 62-64] and manufacturing processes simulation software, DEFORM-2D/3D [3, 30, 65-70]. These software have dedicated machining modules those offer systematic and simple setup for the development of 2D and 3D machining models which have simplified the modelling process for the end-user. Other notable software used for machining includes Forge2 [71-73] and NASTRAN.

There are certain advantages and limitations of general-purpose software as well as specialized machining software based on modelling techniques, the accuracy of results and computational performance. Various studies have been performed to compare the performance of FE software in the chip formation process [74, 75]. The introduction and comparison of software based on modelling methods are briefly discussed below.

2.1. AdvantEdge

AdvantEdge is a FEM based explicit machining software developed by Third Wave System and offers a machining-specific user interface for 2D and 3D models. Since

6

AdvantEdge has specifically been designed for machining purposes, implementation of chip separation criteria is not required in the presence of Lagrangian based adaptive meshing feature to reduce the mesh distortion. The package has a built-in editor for tool geometries and coating conditions and also provides the option to import geometries from other modelling software [76, 77]. The program also offers an extensive material library for metals and alloys. Other constitutive models can be implemented using user-defined subroutines. Although the program has been widely used to simulate metal cutting, it does not offer support for composite or brittle materials. Another important feature of AdvantEdge is a defined setup for tool life analysis and residual stress modelling.

2.2. DEFORM

DEFORM (Design Environment for Forming) was developed by Scientific Forming Technology company (SFTC) for manufacturing operations. Initially, DEFORM-2D was developed for 2D manufacturing simulations with the later addition of DEFORM-3D for 3D modelling. The software is based on an updated Lagrangian formulation which uses an implicit integration scheme to handle large deformation during machining simulations. It also offers a selection of popular cutting tool and tool holder models in a database with the flexibility to model new geometries [78]. Both tool and the workpiece can be modelled as deformable bodies and solution variables can be obtained for both tool and workpiece. Although the package has extensively been used for forming operations, it has also been successfully used to model turning [3, 33, 65, 66], milling and drilling as well as for tool wear studies [69]. DEFORM offers a good selection of material libraries and some tool geometries along with the flexibility to introduce user-defined material data.

7

2.3. Abaqus

Abaqus is general-purpose FEM software developed by Simulia to address a wide range of problems. Abaqus does not offer any dedicated module for machining and, therefore, the user must manually model tools and workpiece geometries. The software offers a variety of user-subroutines to introduce and evaluate new constitutive material models [55], friction criteria, tool wear, and other related machining conditions.

Abaqus software consists of three main products: Abaqus/CAE, Abaqus/Standard and Abaqus/Explicit. Abaqus/CAE is an interactive module that integrates the solver modules into CAE (Complete Abaqus Environment) for modelling, analysis, job management and offers inclusive tools for results interpretation and visualization. Abaqus/Standard offers analyses of static and dynamic implicit problems for solving smooth non-linear problems. However, the convergence of such problems may be difficult, due to contact or material complexities (e.g., large deformation) and many iterations may be needed to obtain a converged solution. On the other hand, Abaqus/Explicit finds the solution without iteration by advancing the kinematic state from the end of the previous increment being capable of tackling high-speed non-smooth non-linear problems efficiently. Although Abaqus/Explicit is the most suitable solver and has been used extensively for machining simulations, some researchers also exploited Abaqus/Standard for such simulation.

Abaqus also facilitates the use of particle methods including smoothed particle hydrodynamics (SPH) and discrete element method (DEM) as well as feature of conversion of elements to SPH particles during the analysis. However, the software does not offer a proper interface to design particle-based machining simulations and,

8

therefore, the generated input files are required to be modified to simulate the particle-based analysis.

2.4. LS-DYNA

LS-DYNA is a general-purpose implicit and explicit FEM software developed by Livermore Software Technology Corporation (LSTC) to analyse linear and nonlinear behaviour in 2D and 3D analysis. The software offers a comprehensive material library which includes metals, plastics, ceramics, and concrete. It also offers a facility to create the user-defined material models. as well as it provides user-defined material capability. LS-DYNA has been employed in various metal cutting simulations and offers a wide range of particle methods to simulate the machining processes [57, 79]. The software provides an advanced interface to simulate the process using particle methods and it can be considered as the most advanced software for particle-based machining simulations. Due to the inclusion of meshless techniques including SPH and DEM, the software has found a great potential in the development of more realistic models for cutting of hard and brittle materials [80].

2.5. Marc

Marc is a general-purpose FE software developed by MSC Software also employed for machining simulations. It offers the capability to simulate 2D and 3D machining processes [60, 81]. The software also provides an extensive choice of elements and material library for a wide range of materials with the flexibility to introduce a user-defined material model. Various plasticity and failure models are integrated to simulate material response behaviour including plastic deformation and brittle fracture. The adaptive meshing feature can be exploited under extreme mesh distortion conditions and user-defined mesh control can be implemented.

Table 1 presents the comparison of FE software with its advantages and disadvantages in developing a machining simulation model.

Table 1: Comparison of FE software based on machining modelling features				
Software	**Machining module**	**Formulation & Analysis**	**Advantages**	**Disadvantages**
ADVANTEDGE	Turning, milling, drilling	LAG (Adaptive) Explicit	Machining specific user interface, Simple control, Built-in editor for tool and workpiece, ductile material library	Very limited user control, can't simulate all materials, limited elements and material types,
DEFORM	Turning, milling, drilling, forging,	LAG (Adaptive) Implicit	Machining module, Easy setup, extensive material library,	Limited user control, limited element type
ABAQUS	General-purpose (No machining module)	LAG, EUL,ALE,SPH,DEM,CEL Implicit/Explicit	High user control, can simulate any machining operation, extensive element library, modelling freedom, online conversion to particle	No machining module, time-consuming setup, difficult mesh design, no material library, 3D SPH only
LS-DYNA		LAG,EUL,SPH,DEM,PFEM,EFG Implicit/Explicit	SPH interface, wide element library, high user control, 2D and 3D SPH capability	Limited modelling control, time-consuming setup
Marc		LAG, EUL Implicit/Explicit	Material library, wide element library, high user control, automatic remeshing	Limited evaluation, time-consuming setup,

3. Finite element formulations

The correlation of continuum and the computational mesh of the problem domain is based on the type of continuum and its dynamics as well as the deformation scale. The three main relative motion algorithms or numerical formulations developed and adopted for machining simulations are the Lagrangian approach, Eulerian approach and Arbitrary Lagrangian-Eulerian (ALE) approach.

3.1. Lagrangian formulation

The Lagrangian approach has widely been adopted in cutting simulations due to its numerical accuracy. In the Lagrangian approach, both elements and nodes of the

mesh remain attached to the material, and it is easier to apply boundary conditions and track free surfaces. Lagrangian mesh deforms mimicking the deformation of the underlying material such that the position of mesh nodes relative to material points remains fixed. The Lagrangian approach in machining simulation has been extensively used [45, 82-87] since its earliest implementation in 1973 by Klamecki [88].

One of the limitations of the Lagrangian approach is severe mesh distortion due to large deformations inherent in cutting simulations. The excessive element distortion at the tool-chip interface lead to convergence errors and termination of the simulation. Modelling chip formation requires node separation by using adaptive meshing or chip separation methods. Also, when using negative rake angle tools and round edged tools, the node separation methods suffer performance failure [89]. Further categorization of the Lagrangian approach is based on the interrelation of nodes and classified as mesh-based and mesh-free methods.

3.2. Eulerian formulation

The Eulerian approach has been adopted in machining simulations of metals. In the Eulerian formulation, mesh remains fixed in space and material is allowed to move through the mesh during deformation. Since the mesh boundary nodes and intrinsic material boundary nodes may not be coincident, it is difficult to model free boundary and interface conditions. When using the Eulerian approach for cutting simulation, chip geometry needs to be defined beforehand.

The pioneer works of the Eulerian approach in cutting simulation was done by Usui et al. [90-92]. Carrol and Strenkowski [93] adopted Eulerian formulation in viscoplastic cutting simulation and their model is known as the Eulerian cutting model. They also developed an orthogonal cutting model for the single point diamond turning process

11

[21]. Although they found the model to be more accurate and computationally efficient than the updated Lagrangian approach, it was difficult to predict the final chip geometry. Later Strenkowski and Moon [94, 95] improved the model by employing a free surface algorithm to determine final chip geometry and tool-chip interface length. A good percentage of FE machining simulations work using Eulerian formulation has been conducted to evaluate chip geometry and to optimize many other machining variables [6, 96, 97].

The Eulerian approach offers a solution to the mesh distortion exploiting fixed reference frame and a predefined chip geometry is required to simulate the cutting process. Since the geometry of the chip influence other machining variables including friction, temperature and cutting forces; an improper predefined chip geometry leads to misleading results. The Eulerian approach is more appropriate for fluid simulations or in processes where material boundaries are already known and well described. The approach has been successfully adopted in forging and extrusion processes [98].

The Eulerian approach has some precedence over the Lagrangian approach, as it does not suffer from mesh distortion issues and, therefore, no remeshing is required. It also offers direct steady-state solutions without undergoing a transition from incipient to steady-state conditions for accurate solutions and therefore computationally less expensive.

3.3.   Arbitrary Lagrangian-Eulerian formulation

The ALE approach exploits the benefits of both classical Lagrangian and Eulerian formulations. ALE allows the boundary nodes to be coincident with material boundaries while adjusting interior nodes to reduce mesh distortion. In cutting simulations, ALE maintains the Lagrangian capability of constrained mesh motion at

free boundaries while maintaining the Eulerian behaviour during chip formation in the high deformation zone. Retaining the capabilities of both approaches in ALE formulation resolves the problem of mesh distortion along with exploiting natural chip formation without predefining chip geometry. The implementation of the ALE approach involves the adoption of user-defined mesh regularization or mesh-adaptation strategy [99]. The mesh regularization techniques ensure that the mesh is regular during high deformation, by continuously updating the nodal coordinates using displacement or velocity parameters. The estimation of a problem solution domain using the ALE approach can be achieved either by concurrently solving all non-symmetric equations or by using the ALE operator split method to decouple Lagrangian equations [40]. ALE with mesh adaptation approach involved localized mesh refinement within high deformation zone and remeshing.

Many researchers used ALE formulation in machining simulations to evaluate ALE formulation for cutting simulations as well as in different machining analyses including chip formation study and the effect of tool geometry with varying input variables representing the machining condition [25, 40, 67, 100-103]. ALE approach can be employed with Lagrangian boundaries [67, 104] as well as Eulerian boundaries [8, 103] in the chip formation zone (Fig. 2).
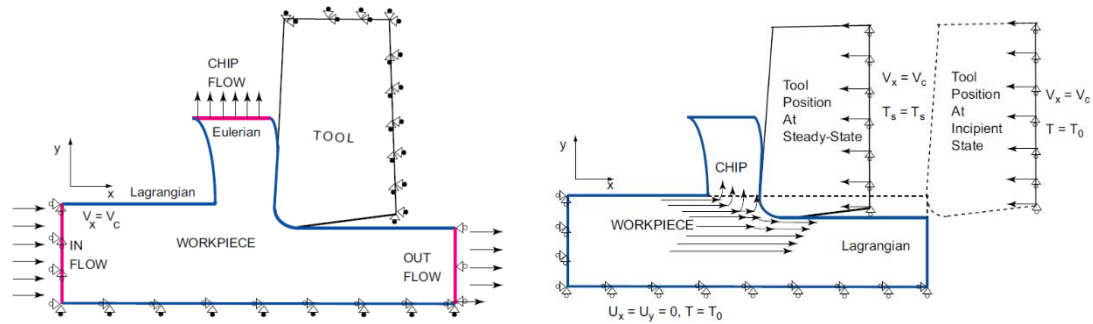
Fig. 2: ALE formulation with Lagrangian and Eulerian boundaries (left),
Lagrangian only (right) [61]

When using ALE formulation with Eulerian boundaries, the friction criteria at the tool-chip interface do not significantly influence the output variable compared to the model results based on the ALE formulation with Lagrangian boundaries [67]. ALE formulation with predefined chip shape has also been studied by many researchers. Movahhedy et al. [25, 100] and Olovsson et al. [101], evaluated the performance of ALE in 2D cutting simulations and reported that no chip separation criteria is required using this approach and results can be better predicted than with the Eulerian technique alone. Various tool wear numerical simulation studies are also based on the ALE formulation [105-108].

4. Particle-based formulation

Particle methods were developed to approximate the problem domains involving the interaction of fluids and solids. Difficulties involved in using the Eulerian and ALE approach to simulate the interaction of the fluid with different multiple bodies leading to the use of Lagrangian formulations as a preferred choice. Particle methods, in general, can be classified as mesh-based or meshless methods. In meshless methods, the definition of shape functions is only dependent on node positions with no connection required between the nodes of the problem domain. Also, all the mechanical and thermal properties including density, velocity, temperature are

14

assigned to the node itself rather than mesh elements. In mesh-based particle methods, nodes at the intersecting elements behave like particles and move during deformation with their physical properties. Remeshing occurs according to the new position of the nodes during each time step. Thus, mesh-based formulation exploits the features of meshless approach and FEM.

Various particle methods developed mainly for the fluid dynamics simulations have successfully been adopted in machining simulation including Smoothed Particle Hydrodynamics (SPH) [109], material point method (MPM) [110], particle finite element method (PFEM), and Finite point-set method (FPM). The main differences between these particle methods are the mesh features and type of interactions between the particles as well as the calculation of the relative position of a particle of interest and its neighbouring particles.

All the meshless methods offer common advantages and disadvantages over classical FEM. The main advantages of these methods over FEM include: (1) Meshless methods are based on Lagrangian formulations and, therefore, offer better approximation in cutting simulation problems over both Eulerian and ALE based techniques (2) No artificial physical or geometrical separation criteria is required for chip formation as required in Lagrangian mesh-based FEM (3) Remeshing is not required using the mesh-free approach. The main disadvantages include: (1) Mesh-free methods are computationally more expensive than conventional FEM due to a high number of neighbouring particles (2) Meshless methods are not fully developed for all types of analysis for cutting simulation processes and further development is needed (3) Meshless methods are less sensitive to small deformations in comparison with FEM and, therefore, less efficient than FEM for small deformation problems.

15

4.1.   Particle Finite Element Method (PFEM)

The PFEM method was developed to solve fluid-structure interaction problems including dynamic free surfaces, flow separations, collapse situations and other general fluid mechanics problems [111, 112]. The basic modelling of fluid and solid domains in PFEM is based on updated Lagrangian formulation. The discretization of fluids and solid domains is done by FEM using mesh generation based on extended Delaunay tessellation (EDT) [113]. The key feature of the PFEM method is the very fast mesh generation at every time step based on node position in space using the EDT method. The PFEM method adopts MFEM (Meshless Finite element method) [114] shape functions to solve incompressible Navier-strokes equations to evaluate forces on each particle.

The implementation of the PFEM method was later extended to assess surface wear situation [113], in the analysis of fluid-multibody interaction [115], modelling of bed erosion in free surface flows [116] and other fluid dynamic problems. The application of PFEM for cutting process simulation was first proposed by Oliver et al. [117]. Later Carbonell [118] used this approach to model the tunnelling process and tool wear in rock cutting. Sabel et al. [119, 120] performed the tensile test and cutting simulations tests using PFEM and compared the results with FEM simulations. They found the approach useful for machining simulations. Rodriguez et al. [121] performed cutting simulations to evaluate PFEM as an efficient numerical simulation tool for the cutting process. They conducted orthogonal cutting of 42CD4 steel using PFEM and analyzed output variables including cutting forces, stresses, strains and temperature and compared the results to the experimental results as well as numerical cutting simulation results using Abaqus, AdvantEdge and Deform. Furthermore, they performed sensibility analysis to geometric and cutting conditions of PFEM usability

16

using the Design of Experiments (DoE) methodology. They found some results in good agreement with experimental and other numerical simulation studies and some discrepancies. They concluded PFEM as an efficient approach that could approximate better solutions to cutting simulation problems and, therefore, required further development and evaluation for different machining processes.

4.2. Finite point-set Method (FPM)

The FPM developed by Fraunhofer Institute for Industrial Mathematics (ITWM) is a mesh-free numerical method to simulate mechanical and fluid dynamics problems [122]. The FPM is based on the law of conservation of mass, energy and momentum and exploits the finite difference method (FDM) and moving least square method to solve differential equations and approximation of field value and derivatives respectively [123]. In FPM, similar to the SPH approach, each particle produces a sphere of influence and interacts with other neighbouring particles within a smoothing length. Any undesired particle accumulation or cavities can be avoided by deleting or generating particles using an advanced particle management algorithm. This method was successfully employed for the cutting simulations of medium carbon steel AISI 1045 and nickel-based alloy Inconel IN718 for continuous and segmented chip formations and compared with experimental and DEFORM simulation results [123, 124]. Although some results were found in good agreement with experimental and other simulation studies, certain discrepancies were observed in thrust forces, shear angle, temperature, and chip geometry. The method is still in the development stage and not much further work is published using this approach.

17

4.3.   Discrete element method (DEM)

Another popular addition to meshless methods is DEM with a wide range of applications in many different fields. The DEM was originally developed by Cundall in 1971 to solve geomechanics problems [125] and since then gradually and continuously evolved through various development stages. The DEM model consists of discrete or detachable solid rigid particles initially glued together. The particles can be of different 2D or 3D shapes and sizes including circles, spheres, triangles polygons, ellipses, and many more [113]. The contact forces between the particles are governed by relative displacement based on force-displacement law [126]. A DEM based software package PFC2D was mostly used to simulate different machining processes. A typical DEM simulation includes three main stages namely, pre-processing, dynamic calculations and post-processing. Calibration methods based on the unconfined compressive test, Brazilian test, three-point bending test and fracture toughness tests are generally conducted to calibrate the particle properties [127, 128]. One of the earliest applications of DEM in orthogonal cutting simulations was performed by Fleissner [129] using spherical particles. Qui et al. [128] performed indentation and 2D and 3D cutting simulations to investigate the machining mechanism of glass and tool geometry effect. The authors claimed that their results were not compared with any experimental study or other established numerical simulations approach. Tan et al. [126, 130] employed DEM to investigate crack initiation and propagation in Al_2O_3 and SiC at micro-scale and compared the results with experimental studies. Lliescu et al. [131] performed an orthogonal cutting simulation of carbon fibre reinforced polymer. Eberhard and Gaugele [127] performed an orthogonal cutting simulation of steel and aluminum using DEM and compared it with experimental results. However, the results obtained were not satisfactory in terms

18

of chip geometry and cutting forces. They also pointed out the dependency of material model parameters on particle size, geometry and arrangement which is a major drawback.

4.4. Smoothed Particle Hydrodynamics (SPH)

SPH is the earliest developed and most frequently adopted method for machining simulation among meshless particle methods. SPH approach was first developed by Gingold and Monaghan in 1977 [109] for astrophysics applications. SPH uses a kernel approximation to approximate field variables and properties in the domain as shown in Fig.3.
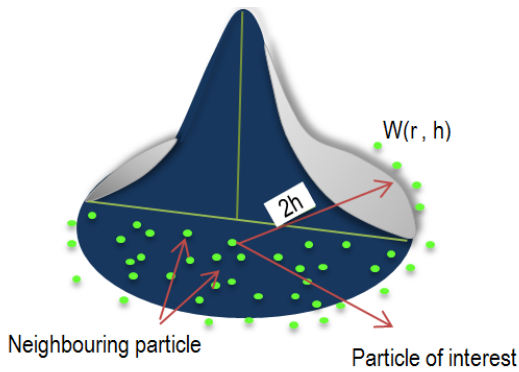
Fig. 3: SPH kernel approximation

SPH approximates field variables at any particle by classical summation of smoothing function values of neighbouring particles within a sphere of influence. The length that defines the sphere of influence is based on smoothing length and it is the maximum distance to which the interaction can occur, and it is defined as $f(x) \cong \sum_{j}^{\infty} \frac{(m_b)}{\rho_b} f_b W(|X - X_b|, h)$ where, $f(x)$ is a scalar function and subscript b represents the neighbouring particle of a particle *for* which field variables need to be approximated. W is a smoothing Kernel function with radius h, called the smoothing length. m_b and ρ_b are mass and densities of b particles. X_b is the location of particle b

19

with its value f_b. In the SPH method, all particles have a physical degree of freedom and each particle movement is influenced by its neighbouring particles located within the sphere of influence of radius r which is two times the smoothing length, $2h$. The particles beyond the area of influence do not contribute to the intrinsic property of cohesion on the particle of interest. In SPH formulation, particles interact with each other based on defined constitutive equations. SPH has successfully been used in metal forming [132], metal cutting [17, 57, 133], indentation [134], fracture mechanics [135], geo-mechanics [136] as well as in structural mechanics [137] studies.

In comparison with FEM, the SPH approach is found less efficient in studying processes with tensile instability [138, 139] or small deformation processes. Nevertheless, it has been found more effective to study large deformation processes when compared to Lagrangian mesh-based approaches to model the same. SPH approach has also been found to perform analogously to FEM following sensitivity analysis of particle resolution, mass-scaling and reported to be better than FEM in interface friction criteria [140]. In metal cutting processes, the SPH method was used for studying chip formation of soft metals such as copper [17, 141], aluminium [133, 142] as well hard materials such as titanium alloys [143] and brittle materials [144]. Limido et al. [57] conducted a comparative study of chip morphology of aluminium alloy and steel using the 2D SPH approach, classical Lagrangian FEM and experimental approach. They found realistic chip formation and proportional cutting forces using the SPH approach for both materials. Madaj and Piska [133] found a good correlation of chip geometry in experimental and SPH simulation of aluminium alloy while investigating the effect of material model parameters and particle density. Calamaz et al. [145] employed the SPH approach to understand the effect of tool wear on the variation of chip formation of titanium alloy Ti6A14V and experimentally

20

validated the results. Table 2 presents the comparison of classical FEM approaches and particle methods based on performance analyses in machining simulations.

Table 2: Performance comparison of approaches for machining studies

Formulation	Type	Advantages	Disadvantages
Lagrangian	Classical FEM	Better results approximation	Chip separation required, mesh distortion, difficult to mesh complex geometries,
Eulerian	Classical FEM	No chip separation required, direct steady-state chip conditions, computationally efficient	Required predefined chip geometry, difficult to locate free surfaces
ALE	Classical FEM	Combine features of Lagrangian and Eulerian, avoid mesh distortion,	Computationally expensive, difficult to apply for brittle materials, remeshing required in extreme deformation, suffer error in history of state variable, inefficient in small deformation areas
SPH, DEM, FPM (Lagrangian)	Particle (meshless)	Particle based (no mesh distortion), better interface friction criteria, Ideal to simulate brittle behaviour	Not suitable for smaller deformation, suffer tensile instability,
PFEM (Lagrangian)	Particle (mesh-based)	Uses features of particle and mesh-based approach, no chip separation criteria required, new mesh adjustment according to node positions,	Computationally expensive, limited performance evaluation

5. Modelling and design of machining simulations

In machining, depending on the type of workpiece, tool material and cutting conditions, cutting temperature could rise to 1500°C or more, with strains reaching a range of 1 to 5 and strain rate ranging around 10^3 s^{-1} to 10^6 s^{-1}. Although FE simulations of machining processes encompass mechanical and coupled thermo-mechanical analysis, thermal effects along with mechanical effects define true machining behaviour. The FEM ability of coupled mechanical-thermal process simulation defines interdependence of perceptible and imperceptible elements of the mechanical and thermal processes. The Design of Experiments (DOE) approach using the Taguchi

21

method or Response Surface Methodology (RSM) adopted in designing experimental machining [82, 146-149] can also be employed for the optimization of the FE machining process. However, a major part of FE machining simulations is based on the general simulation approach without employing any design methodology.

5.1. Machining models and chip formation zones

FE cutting simulations are based on orthogonal and oblique cutting models. In orthogonal cutting, the cutting edge of the tool is perpendicular to the cutting velocity. In oblique cutting, the tool cutting edge is inclined at an acute angle to the direction of the tool. Although most of the machining processes are based on oblique cutting, mostly FE cutting employed by the researchers are based on orthogonal cutting. Comparatively, fewer attempts have been reported on modeling and simulation of oblique cutting [33, 150-153] due to complexities involved in the modeling of chip formation. Both of cutting models produce different chip geometry, chip direction and cutting forces.

In the experimental and mathematical analysis, the development of material separation or chip formation is analyzed in three deformation zones. These zones are identified as primary shear zone (PSZ), secondary deformation zone (SDZ) and tertiary deformation zone (TDZ). The PSZ encompasses from the tip of the cutting tool to the area/point of the free surface where the deformed chip transforms to undeformed chip. The PSZ encompass shear plane or zone and major material shear deformation realize within this zone. The SDZ embraces along the rake face of the tool from the point above the tooltip to the contact length. The TDZ lies from under the tool tip along contact length towards the flank side of the tool. The tool-chip contact area during chip formation is divided into two regions known as the sticking region and

22

the sliding region. Fig. 4 presents the schematic of three deformation zones and sticking and sliding regions.

L_s = Length of Sliding region

L_t = Length of sticking region

$\emptyset_s$ = Shear plane angle

t_{uc} = uncut chip thickness
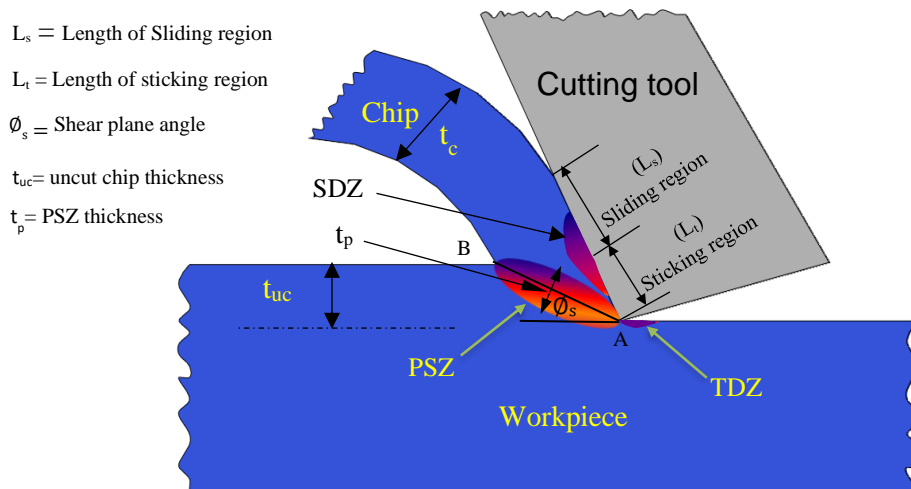
t_p = PSZ thickness

Fig. 4: Chip formation zones and contact region (PZS- primary shear zone, SDZ- secondary deformation zone and TDZ- tertiary deformation zone)

5.2. Defining parts geometry, properties and contact

Regardless of modelling and analysis capabilities of FE software, a typical FE machining simulation involves modelling of tool and workpiece geometries, assigning material properties, meshing the parts, defining tool-workpiece contact properties and boundary conditions as well as selecting the output variables according to the machining analyses. Dependent on the FE software, the parts geometries can be modelled, loaded from the existing database, or imported from other modelling software. In machining simulations, the tool can be modelled as a rigid or deformable body whereas it is required to model a workpiece as a deformable body. The performance of the FE machining model and to accurately predict the true material response behaviour of the deformed material is highly dependent on assigning the appropriate material properties with relevant plasticity and damage models. Properties including thermal conductivity, specific heat, and thermal expansion are required while performing coupled thermo-mechanical analysis.

23

The contact modelling of the tool and workpiece is the most important factor that governs the accuracy of chip formation. A master-slave approach has frequently been adopted [154] in which master surface and slave surface are in contact with each other. In principle, rigid surfaces or harder materials are generally considered master surfaces and deformable or softer bodies as slave surfaces. This selection is important since the master surface can penetrate slave surfaces while the reverse is not allowed. Fig. 5 presents an example of the penetration of the master surface into the slave surface.
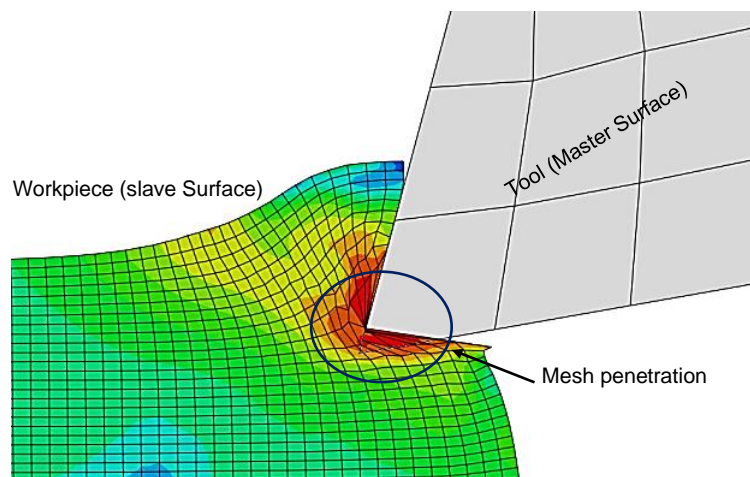
Fig.5 Penetration of master into slave

Nodes or surface contacts can be defined between the tool and workpiece surfaces dependent on formulation and cutting conditions [155]. The friction models as well as tangential (frictional) and/or normal contact behaviour with/without heat generation can be selected dependent on the available model in employed FE software. Kinematic or penalty contact method with finite or small sliding can be applied to represent the tool-workpiece contact [67]. To simulate the chip separation, it is important to define the contact at the internal nodes rather than only on the external surfaces of the workpiece.

5.3. Meshing or discretization

In FEM, due to complex parts geometries as well as the need to analyze the distribution and intensity of output variables within specific domains, continuum structures are divided into elements interconnected to each other at the intersection points called nodes. The discretization involves subdividing the problem domain into finite elements of different sizes and shapes. The meshes of workpiece and tools in machining simulations are based on 2D or 3D elements. The earliest 2D FE cutting simulations studies were based on 2D linear triangular elements and later followed by quadrilateral elements [82]. The advancing front method and the Delaunay triangulation methods [154, 156] are the basis of many mesh generation programs for meshing. Using the Delaunay triangulation method, only triangular elements can be used for mesh generation.

The performance of chip formation and the severity of mesh distortion in the Lagrangian formulation are highly dependent on the type of elements used [157] which can influence convergence and numerical stability. The performance of elements can be influenced by the cutting conditions, tool geometry and cutting speed with respect to the type of machining. The same element configuration offers varied elements efficiency under two different cutting conditions. During the deformation, elements suffer two major numerical problems called shear locking and volumetric locking. Finite elements endure locking if faced with an artificially stiff response to deformation. One of the main reasons for locking is the inability of interpolation functions to approximate strain distribution accurately in solids. Another possible factor that leads to the locking problem is an improper FE equation system caused by poor governing equations.

25

Second-order elements are considered as they yield accurate results in machining simulations when compared to first-order simplex elements which often suffer from volumetric and shear locking during deformation [154]. The first order fully integrate quadrilateral elements offer better convergence properties than triangular elements in orthogonal cutting [26, 158]. The fully integrated elements and elements with reduced integration show dissimilar deformation behaviour under extreme deformation conditions. The degree of chip segmentation was found higher when using fully integrated elements [26, 158]. When modelling continuous chip curvature, fully-integrated elements offer better curvature than reduced-integration elements [54]. The elements with full integration have more affinity to undergo volumetric locking. Although the implementation of reduced integration in quadrilateral and brick elements could be helpful to avoid the locking phenomenon, it also suffers locking when using 4-noded quadrilateral or 8-noded brick elements [82].

The number of elements within the unit area refers to mesh density dependent on the element type. Although mesh density is crucial in achieving ideal chip formation with better results, the computational cost could be higher using the same mesh density within the whole domain. It is advisable to use refined mesh in and near chip formation zone while coarse mesh can be used in the remaining model.

6. Chip formation and separation methods

Controlled material removal also known as chip formation is a complex phenomenon in machining simulations. The three main chip morphologies researched in 2D and 3D FE cutting simulations of metals are continuous chips, discontinuous or broken chips and segmented or serrated chips. The final geometry (shape, length, thickness, width) of all these chips is dependent on employed FE formulation (element-

26

based, particle-based, ALE amongst others), mesh quality (element type, density, orientation, etc.), chip separation criteria, and cutting conditions (speed, feed, depth of cut,). In general principle, continuous chips are obtained by plastic deformation without fracture in the form of a coil or slightly curved form, dependent on material ductility [159]. However, FE cutting simulations are based on two conflicting theories for the initiation of continuous chip formation. One theory of inception of chip formation is based on crack generation ahead of the tool tip and its propagation with the cutting speed [160]. The other theory doesn't support any crack formation ahead of the cutting tool tip [28]. Discontinuous chips are mainly obtained by brittle fracture (removal by cracks) or chip breakage in the secondary deformation zone. These chips are obtained in completely broken segments of different shapes and sizes and generally formed in the machining of brittle materials. Serrated chips appear in segments loosely attached to each other in the saw-tooth form on the free surface of chips. These chips are obtained by the fluctuation of high shear strain and low shear strain and are normally obtained in hard and brittle metals. This chip formation behaviour is similar in several biomaterials used as dental implants, hip and knee implants [48].

Due to a fixed reference frame, no chip separation criterion is required when modelling using the Eulerian approach. However, due to free material flow through the mesh, predefined chip geometry is required. The pioneering FE studies performed in 1971 by Zienkiewicz [161] and Kakino [162] were the most basic cutting simulation studies using simple predefined chip geometries. Later Shirakashi and Usui [163, 164] developed the basic predefined chip model by introducing an iterative convergence method (ICM) for predicting an optimized predefined chip geometry. The ICM method was used to update predefined chip shape until the obtained plastic flow was consistent with the predicted shape. It was based on updated Lagrangian elastic-

27

plastic analysis which involved: (a) initial guess of a steady-state chip shape with a small crack at the cutting edge to ease chip separation from workpiece (b) tool movement into the chip with first iteration (c) satisfying fully developed plastic flow condition by iteration and (d) the shape of predicted steady-state deformed chip is obtained which correlate the generated plastic flow properties and friction conditions with the tool. Although the developed model was computationally efficient for elastic-plastic analysis, it failed to follow the actual path of chip formation whereas elastic-plastic flow is path-dependent [164]. Under different cutting conditions, the crack may develop a kink, assume a curved path or different shape as it grows. Also, the model cannot be adopted for non-steady-state chip formation analysis. The ICM was later tested and further developed by other researchers [165].

When using the Lagrangian approach, the separation of chip mesh from the workpiece mesh undergoes high distortion due to large deformation conditions in cutting. To resolve Lagrangian mesh distortion during cutting, various chip separation criteria have been developed to facilitate material removal from the workpiece. The classification of these separation criteria is based on physical and geometrical parameters.

6.1. Physical separation criteria

One of the earliest works in the development of chip separation methods to achieve chip formation was done by Strenkowski and Carrol [21, 50]. They developed chip separation criteria based on the effective plastic strain. In their work, chip separation from workpiece was meant to take place once the value of effective plastic strain at nodes ahead of cutting edge exceeds a predefined threshold value. The effective plastic strain threshold value was found to influence the residual stresses and chip

geometry. The value found during their study lie between 0.4 to 0.65 which is dependent on the cutting conditions.

Later, various researchers proposed chip separation criteria based on different physical parameters. Lin and co-authors [22, 166, 167] proposed chip separation criteria based on strain energy density. Zhang [24] used normal failure stress separation criteria while investigating work hardening effect in elastic-perfectly plastic and elastic-plastic with work hardening constitutive models. Hillerborg et al. [168] proposed critical fracture energy required to open a crack and stresses for the evolution of cracks. Hashemi et al. [169] developed a crack initiation algorithm for chip separation and segmentation using principle stress criteria as a function of fracture strength. In their work, when the value of principle stress at nodes reaches a predefined critical value, a crack was initiated ahead of the tool tip. Owen and Vaz [170] investigated chip formation in high-speed machining and employed equivalent plastic strain and uncoupled integration of Lemaitre ductile damage model [171]. Chen et al. [53, 172] proposed energy-based ductile failure criteria based on equivalent plastic strain and element characteristic length along with shear damage criteria for the chip formation. Ducobu et al. [173] proposed temperature-dependent tensile failure criteria based on eroding element method.

Although all these criteria were successfully adopted by later researchers [11, 169, 174-178] the criteria were also reproached as the values of these physical parameters significantly varies with cutting conditions, tool rake angle, cutting speed and feed [24].

6.2. Geometrical chip separation criteria

The earliest chip separation criteria based on geometrical parameter was adopted by Usui and Shirakashi [23] to resolve mesh distortion during chip formation. The

general approach in the geometrical criteria is based on the failure at the critical distance between the nodes present at the line within the dedicated partition layer. Fig. 6 illustrates the geometric separation criterion in which chip formation takes place with the separation of nodes. In this model, when distance D between the tool cutting edge at point (d) and the workpiece node (point $H_{1,2}$) immediately ahead of the tool become less than the predefined threshold value, node separation takes place. It is also required that the value of critical distance D must be small enough to produce chip formation in a continuous mode as well as the value should be optimal to predict true deformation behaviour. Although the implementation of geometrical criteria is simple in machining simulations, to maintain the chip separation direction, there is a need to introduce a predefined separation line to separate linked elements of workpiece and chip. This parting line limits the simulation model to exploit only the sharp edge of tools to integrate with the parting line.
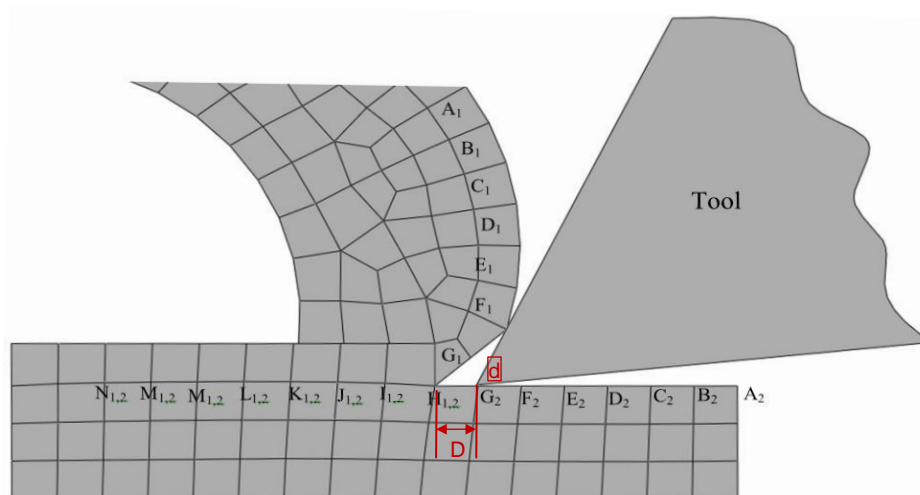
Fig. 6: Chip separation criteria based on geometrical parameter

An improper critical distance value could result in an unrealistic gap of machined material. It also results in convergence and numerical instability problems and greatly influences the authenticity of the results obtained. While investigating the performance

of geometrical and physical chip separation criteria using plane-strain deformation, Zhong et al. [24] found that the critical geometric distance should be sufficiently small (tending to zero) to achieve numerical stability. Komvopoulos and Erpenbeck [83] exploited distance based criteria using plane-strain steady state model and determined the optimal value of critical distance to be 0.5L (half of element length, L) using trial and error simulations. Obikawa et al. [179] used geometric criteria and selected critical distance equal to one-fifth of undeformed chip thickness. Mamalis et al. [61] used geometrical separation criteria in their cutting model and used critical distance equal to 5% of the element length. Zhang and Bhagchi [180] presented geometric criteria along a predefined separation line and proposed the critical distance within 30%-50% of element length. They also introduced improved geometric separation criteria based on the ratio of critical distance to a depth of cut. Later researchers frequently adopted geometrical separation criteria with critical distance value based on material properties, experimental data analysis and cutting conditions [4, 28, 61, 84, 85, 181].

The influence of the critical distance approach on the chip and the machined surface has also been investigated. Movahhedy et al. [25] selected the optimal critical distance value using trial and error cutting simulations. They found that the waviness of the machined surface varies with the change of critical distance value. Huang and Black [182] performed an investigation study to evaluate geometrical separation criteria, physical criteria as well as a combination of both criteria. The study revealed that separation criteria significantly affect stress distribution as well as the distribution of effective plastic strain on the machined surface and the chip. However, the criteria do not significantly influence chip geometry as well as stress distribution in the chip.

The combination of geometrical and physical damage criteria have also been tested for performance and was found to provide better results than individual criterion [19]. Lin and Lin [150-152] employed a combination of strain energy density and geometric distance as chip separation criteria in the oblique cutting model. Shet and Deng [183] and Shih et al. [184] adopted critical stress value as chip separation criteria at a specified distance ahead of the cutting tool. In their model, chip separation occurs when a stress index factor reaches its critical value at a specified distance ahead of the cutting edge of the tool. The stress criterion was defined as:

$$f = \sqrt{\left(\frac{\sigma_n}{\sigma_{fl}}\right)^2 + \left(\frac{\tau}{\tau_{fl}}\right)^2}, \qquad \sigma_n = \max(\sigma_2, 0) \qquad (1)$$

In eq. (1), f is stress index parameter, σ_n and τ are the normal and shear stresses at an assigned distance ahead of the cutting tool. The components σ_{fl} and τ_{fl} are pure tensile failure stress and shear failure stress, respectively. According to their model, when the value of the stress index factor reaches its critical value of 1.0 at an assigned distance (size of one element), chip separation takes place.

6.3. Chip formation based on damage models

Chip separation based on damage models is intrinsically a physical criterion and the critical failure values are based on the relationship of physical parameters rather than the value of the single physical parameter. The specialized as well as general-purpose commercial machining FEM software provide the option to use built-in damage models or allow assimilating user-defined damage model subroutines.

The most frequently adopted damage model for metals in commercial FEM packages is the Johnson's Cook (JC) damage model. The JC damage model [185] has been extensively implemented in machining for a wide range of workpiece

materials [157, 186-191]. The failure criteria of JC damage model are based on equivalent plastic strain at node points of the workpiece. The material failure results in chip separation occurs when the value of damage parameter D_f exceeds 1. The damage parameter of JC damage model is defined as

$$D_f = \sum \left(\frac{\Delta \bar{\varepsilon}^p}{\bar{\varepsilon}_f{}^p} \right), - - - - - (2)$$

where, $\Delta \bar{\varepsilon}^p$ is the incremental change of equivalent plastic strain and $\bar{\varepsilon}_f{}^p$ is the equivalent strain at material failure and is obtained by the following eq. (3)

$$\bar{\varepsilon}_f{}^p = [d_1 + d_2 \exp(d_3 \sigma^*)][(1 + d_4 \ln \frac{\dot{\varepsilon}^p}{\dot{\varepsilon}_0}][1 + d_5 \left(\frac{T - T_{room}}{T_{melt} - T_{room}} \right)], - - (3)$$

where, d_1 to d_5 are material failure parameters, σ^* is the stress triaxiality (hydrostatic pressure (P) to von Mises stress (q) ratio), T is the material temperature and $\dot{\varepsilon}^p$ and $\dot{\varepsilon}_0$ are plastic strain rate and reference strain rate.

6.4. Element deletion method

Chip formation through element deletion has also been adopted by various researchers [19, 192-195] for modelling of continuous and segmented chip formation. In element deletion criteria, the elements in the dedicated layer are deleted when accumulated damage in the zone exceeds the predefined threshold value. The problem with element deletion approach is a loss of volume which is against the law of continuity. To avoid and reduce the volume loss influence, the mesh density needs to be kept significantly higher.

33

6.5.   Remeshing Criteria

One of the solutions proposed to resolve the mesh distortion problem in orthogonal cutting includes the development of remeshing strategies without the need for geometrical or physical separation criteria. Adaptive remeshing introduces new smoother mesh when required to reduce element distortion by maintaining the same mesh topology in terms of several elements and nodes. Fig.7 shows the remeshing criteria applied in cutting model and how it improves the chip formation results.
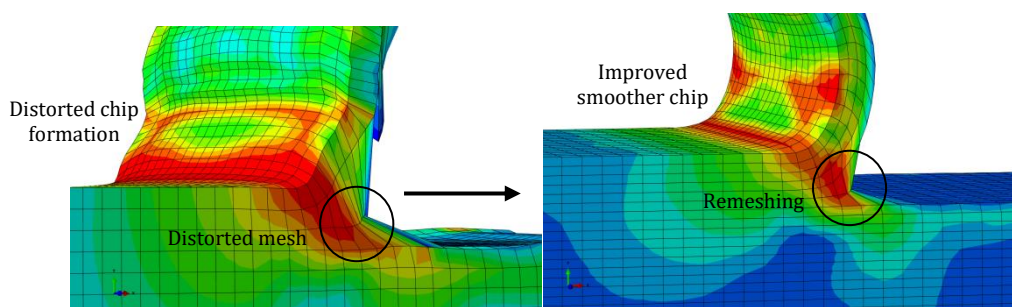
Fig.7: Improved results through remeshing: Old distorted mesh (left), new smoother mesh (right)

In the remeshing technique, when workpiece elements satisfy predefined critical conditions, all the values of state variables are obtained at node points of the distorted mesh by extrapolating the integration point values and averaging over connected elements. A new mesh is generated and all the state variables from the nodes of the old mesh are interpolated to the nodes of the new mesh. However, the transfer of solution variables from old to new mesh could lead to a reduction in the magnitude of variables. This error can be reduced by adopting a more refined mesh in the shear deformation zone during remeshing. One of the issues in refinement is the convergence problem that arises in refining mesh when the position of nodes of the new and old mesh is different [196]. Fig. 8 presents two of the mesh refinement methods used during the remeshing process. In the trapezoidal method, mesh

34

refinement is achieved by geometric refinement using trapezoidal elements with different element angles. In another approach, additional free nodes are introduced within the original mesh by linear interpolation from the adjacent nodes and mesh density can be increased by increasing the number of free nodes and keeping the similar element angle. The choice of mesh refinement criterion is based on deformation conditions and sensitivity requirements.
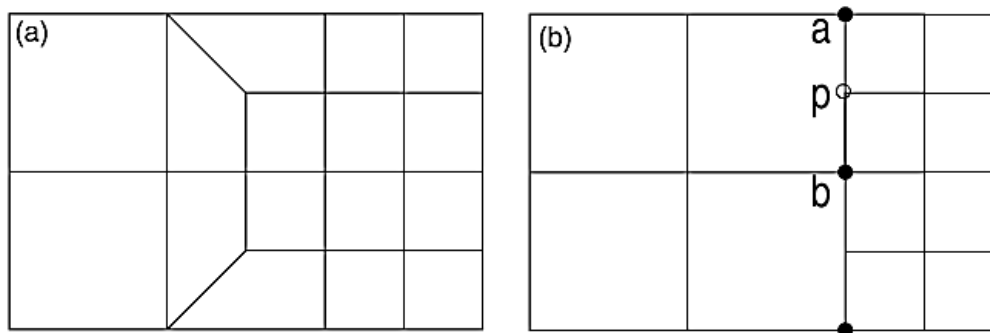

Fig.8: Mesh refinement techniques (a) trapezoidal method (b) additional free nodes of similar angle by interpolation [23]

Remeshing techniques are computationally expensive and frequent remeshing during chip formation could be time-consuming. The refinement during remeshing results in high computational time and accuracy issues. To optimize the remeshing strategy, Shih et al. [28, 85] developed local and global mesh rezoning techniques to improve the computational accuracy and mesh efficiency by refining the mesh ahead of the cutting tool. In their studies [4, 28, 84, 85], they used mesh rezoning techniques which include addition, refinement, combination, and deletion. Fig. 9 illustrates the four mesh rezoning steps adopted in their model explained using dotted lines. The adaptive remeshing initiate when the coarse mesh in front of the cutting tool reaches the proximity of PSZ. In the "addition" step, a new elements column is added toward the front end of the workpiece. During the "refinement" step, the front elements column of the original coarse mesh ahead of PSZ is refined by dividing into two columns. In

35

"combination", two elements column under the tool flank face are combined into one column and in the "deletion" step, the elements column at the back of the workpiece and elements row at the top of the deformed chip are deleted.
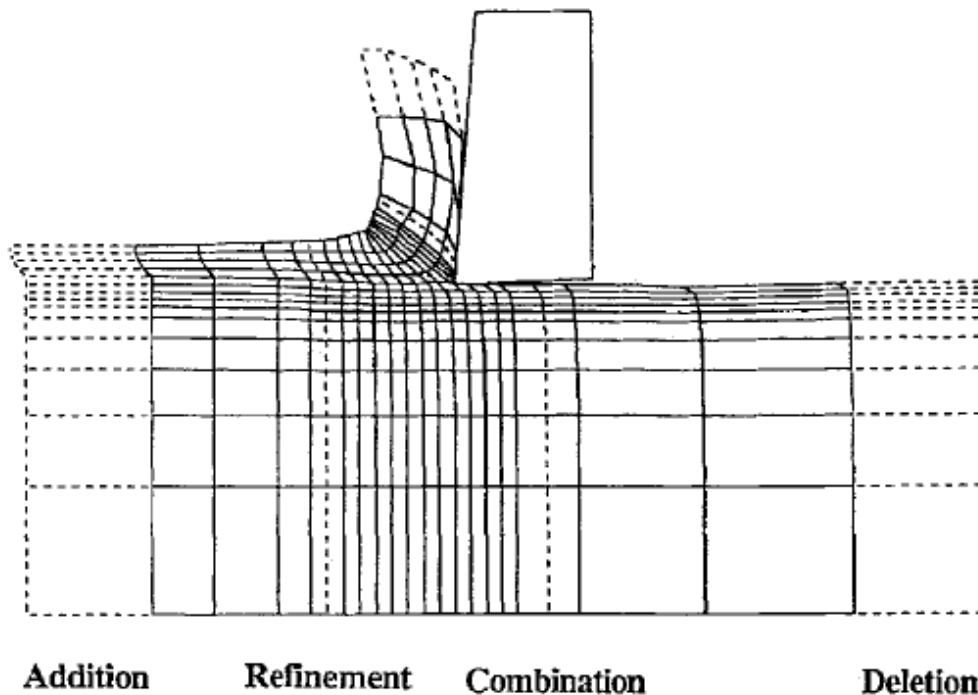

Fig. 9: Mesh rezoning criteria for orthogonal cutting simulation [25]

The most recent development in adaptive remeshing technique considering the secondary cutting edge was proposed by Zanger et al. [29] for 2D and 3D machining simulations. The three critical indicators used in new adaptive remeshing include element's faces corner angle, element's side aspects ratio and deformation degree of elements. In the first stage of their model, the mesh around the distorted elements and within the circle of influence with a predefined radius is deleted. A new part with non-distorted elements of similarly deleted mesh geometry is generated and assimilated into the old, deformed model. The simulation continues with the new integrated part into the original model. Fig. 10 illustrates the stages (a-d) of the developed adaptive remeshing method.
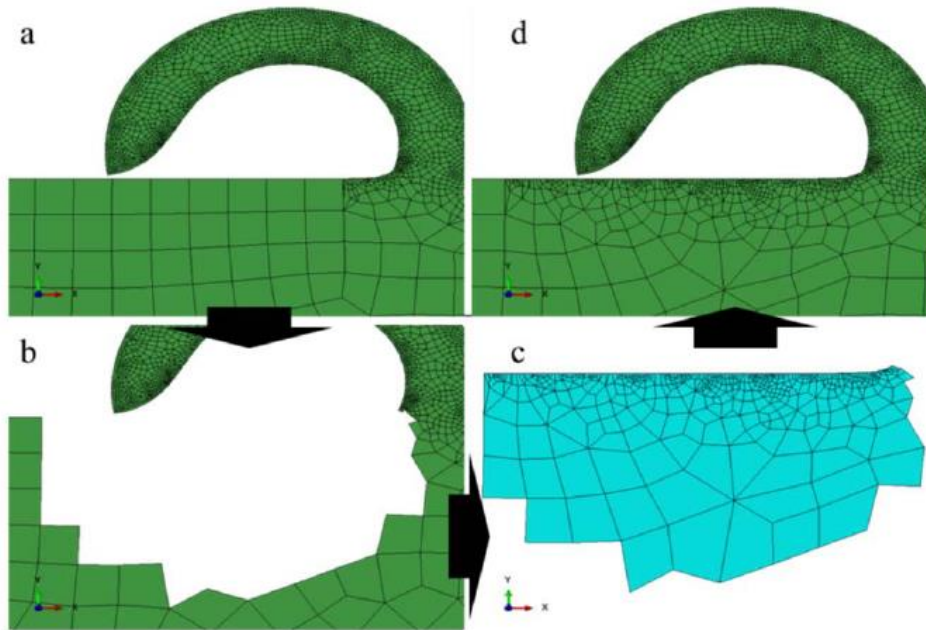
36

Fig.10: Adaptive remeshing based on new part generation [26]

Elements are deleted at stage (b) and a new part with refined mesh is generated at stage (c) which integrates into the old model at stage (d). The deformation degree of elements D was adopted in 3D simulation to reduce the high computational cost and employed as governing rule for both critical parameters of face corner angle and element's aspect ratio using the following equations

$$D_\theta = \prod_{i=1}^{n} \frac{\theta_i}{\theta^{un}} - - - - - (4)$$

$$D_l = \prod_{i=1}^{n} \frac{l_i}{l_i^{un}} - - - - - (5)$$

In eq. (4) and eq. (5), the parameters θ and l represent the number of element corner angles and length of element edges respectively. The scripts i and un represent the conditions of the parameters at the current state and initial undeformed state respectively. Based on these rules, the D_θ and D_l are used to predict the degree of element distortion at subsequent increments. The low-quality elements with a

constant degree of deformation (predicted to undergo no further deformation) are ignored during the remeshing step. This significantly reduces computational time as compared to conventional adaptive remeshing techniques. This approach also solves the issue of volume loss using the element deletion approach.

Adaptive remeshing was employed by various researchers in continuous chip formation [154, 197, 198] as well as in segmented chip formation studies [199]. Sekhon and Chenot [27] introduced an adaptive remeshing model for orthogonal cutting simulation based on geometrical consideration using flow formulation and 6-noded triangular elements. However, they performed rigid-plastic analysis and, therefore, did not include elastic strains during chip formation which significantly influence the realistic behaviour of chip morphology.

The implementation of remeshing criteria is based on remeshing rules that are required to define the mesh control during remeshing. When using the remeshing strategy, it is required to set the critical condition for remeshing. Different remeshing criteria based on critical conditions were adopted by researchers according to different deformation behaviour of mesh elements. A frequently adopted remeshing criteria are based on a change in internal angle of workpiece elements [200, 201] or a combination of internal angle and contact penetration of tool and workpiece elements [202]. Fig. 11 illustrates the method for the estimation of element angle during simulation.
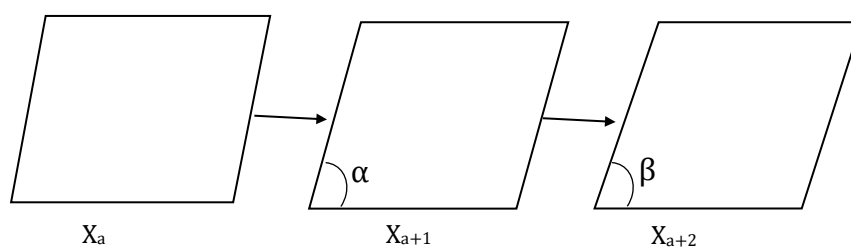

Fig.11: Change of internal angle of workpiece elements

In this approach, the internal angle of elements at any increment is estimated from the internal angle information at the final iteration of the previous increment. At the initial coordinate, X_a and after displacement, ΔU_a of a current increment, the position is estimated by using the following equation.

$$X_{a+1} = X_a + \Delta U_a \; ; \; X_{a+2} = X_{a+1} + \Delta U_a \; ----(6)$$

The step-by-step chip formation takes place by remeshing when internal angle conditions are satisfied. One of the conditions [11, 200, 202] was based on an internal angle is cosα >0.8 and cosβ >0.9 or cosα>0.9 and cosβ>cosα.

Mohammadpour et al. [11] adopted the same remeshing criteria which include elements internal angle, contact mesh penetration with the addition of frequency-criterion. In frequency base criterion, remeshing occurred after every ten increments autonomous to mesh quality. Ng et al. [72] adopted and defined adaptive remeshing criteria in orthogonal cutting which initiate at local penetration rate with the tool edge penetration into the workpiece elements. The remeshing criterion is governed by the correlation of penetrated volume and local penetration rate as:

$$\frac{Vol_i}{v} \times 100 \geq p_l \; ------ (7)$$
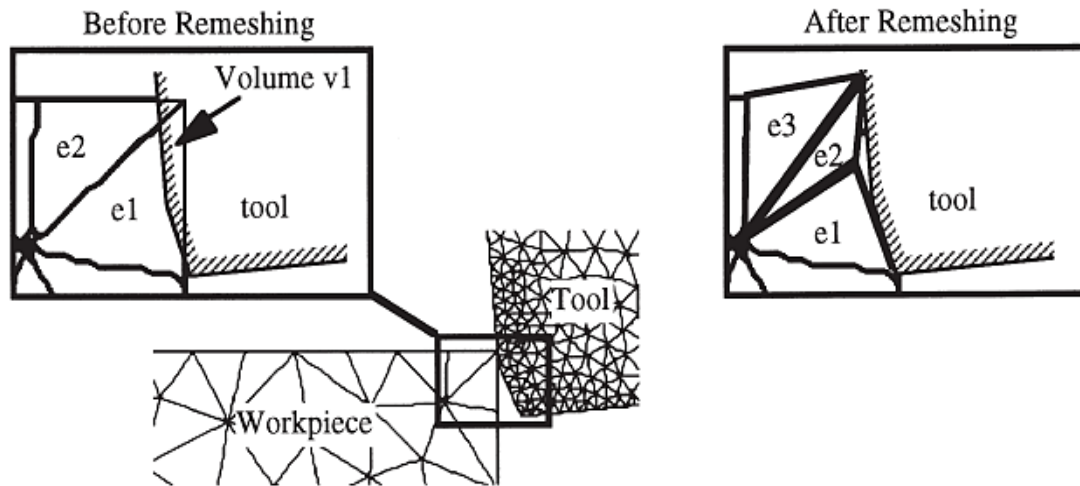
Fig.12: Adaptive remeshing criteria [62]

where Vol_i is the tool penetration volume into the workpiece elements with ith element and υ is the total mesh volume within workpiece and p_l is the local penetration rate. Fig. 12 illustrate the new mesh generation by adaptive remeshing where the remeshing initiate when the tool with volume v1 penetrates element e1.

Although adaptive remeshing technique can be adopted for any material, its performance reduces to failure for brittle and hyperelastic materials. The remeshing technique in comparison with geometrical or physical techniques seems a better strategy for realistic simulation; the results can be affected by crack generation ahead of the cutting (based on the theory of chip formation due to crack) [60]. Although the crack generation and its propagation can be predicted using adaptive remeshing [203], it still suffers some limitations in the estimation of magnitude and direction.

6.6. Modelling of undeformed chip mesh

In addition to geometrical, physical, and adaptive remeshing criteria in chip formations, the initial FE mesh of undeformed chips has been modelled to facilitate chip formation as well as to reduce mesh distortion. Strenkowski and Carroll [50] proposed tilted-elements approach for undeformed chip undergoing large frictional

40

resistance to facilitate chip separation. In this approach, undeformed chip elements are tilted at a certain angle according to the height and width of elements. The approach was later adopted by other researchers using different tilt of elements and shape of undeformed chips based on trials and error or in relation to shear angle [84, 184, 187, 194, 204]. Two of the models adopted by later researchers are presented in Fig.13.
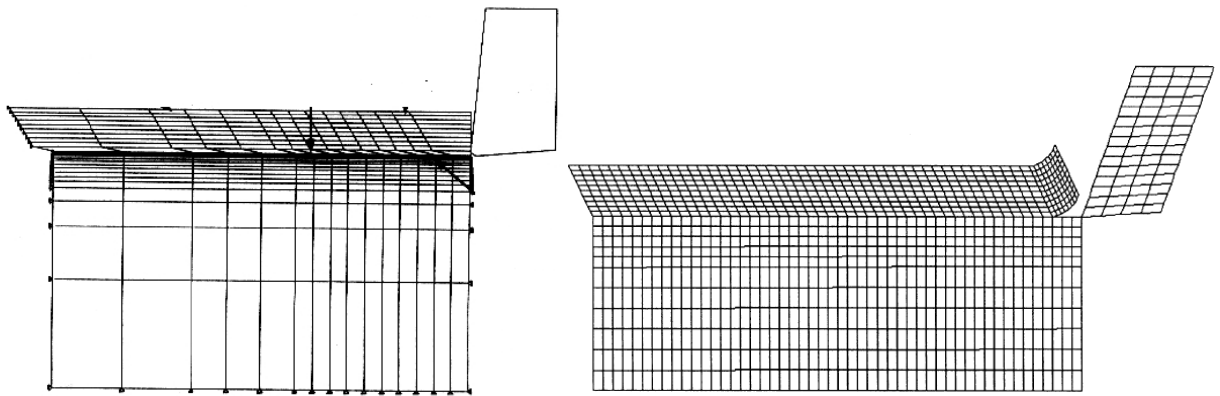

Fig.13: Undeformed chip designs adopted by Shih (left) [69], adopted by Shi (right) [161]

In another effort to optimize chip geometry using the undeformed chip, Baker et al. [26] proposed a "back-mapping" approach to avoid high mesh distortion without frequent remeshing. They suggested that frequent remeshing could be avoided or reduced if elements of undeformed mesh within the chip formation zone are shaped in a warped manner which could offer less distortion. This could be achieved by first designing the mesh and shape of the deformed chip and then from this shape back calculations is performed to achieve the shape of the initial undeformed mesh.
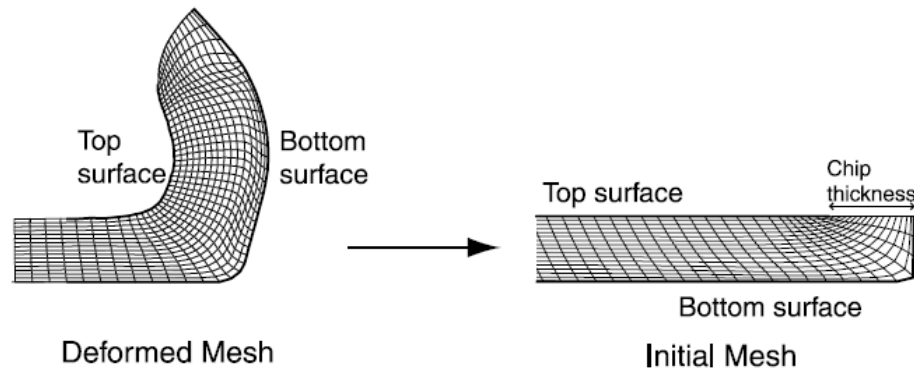
41

Fig.14: Back-mapping from deformed to undeformed initial mesh [23]

Fig. 14 demonstrates the back-mapping approach in which initial mesh is obtained from the deformed mesh with a small number of warped elements. Chip thickness is assumed similar to cutting depth in this example. Although this approach provides a better solution to the mesh distortion problem without any critical value criteria and remeshing, predicting the realistic shape of the deformed chip in advance is difficult. Also, the position of warped elements should be taken into consideration as these elements should lie in a region where they don't significantly influence stress distribution and deformation [26]. The optimized shape could be achieved by designing the mesh and shape of the chip by trial-and-error method.

6.7. Modelling of discontinuous and segmented chips

The formation of discontinuous or segmented chips in a machining simulation is a fundamental requirement to simulate the true response behaviour of hard and brittle materials. The geometry and contour of deformed chips ahead of the tool rake angle influence frictional conditions, cutting forces, cutting temperature as well as tool crater wear. The results obtained in machining simulations of such materials using continuous chip modelling (instead of segmented or discontinuous) leads to misrepresentative material response behaviour. Cutting conditions that influence the type of chip formation should also be taken into consideration. Hua and Shivpuri [205]

42

performed a machining simulation of titanium alloys at different cutting speeds and observed that discontinuous chips are obtained at low cutting speeds whereas, at high cutting speeds, the obtained chips are in serrated form.

The chip segmentation is normally attributed to adiabatic shear (thermal softening) or crack initiation and propagation in a deformed chip or combination of both [26, 155, 206, 207]. The structural transformation of the phase of material has also been recognized to contribute to chip segmentation [208]. Owen and Jr [170] investigated chip formation using physical criteria and a damage model. Their finding suggests chip formation because of thermal softening followed by failure due to strain softening. Thermal softening occurs as a result of high temperature due to localized plastic deformation in a shear zone and strain softening occurs with the initiation and propagation of micro-cracks or flaws. The initiation of cracks was found to develop near the tool tip when using equivalent plastic strain criteria whereas when using fracture strain based on Lemaitre damage model, initiation was found to appear at the free surface of the chip. The chip geometry and ductility [96] as well as cutting conditions [205, 207] also contribute to the location of crack initiation and severity of chip fragmentation. Based on the research studies of chip fragmentation, at low cutting speeds, the crack initiation leading to chip serration mainly occur ahead of the tool tip in the primary deformation zone. However, the crack initiate from the free surface of the chip at higher cutting speeds due to the thermal softening ahead of the tool. Segmentation of the chips has also been found to influence by thermal conductivity. With the increase of thermal conductivity, the degree of chip segmentation was found to decrease [209].

43

Various researchers adopted a combination of physical and geometrical criteria and fracture criteria to simulate segmented chips. A major part of chip segmentation work is based on studies of titanium alloys [173, 205, 210]. Obikawa and Usui [210] proposed a combination of geometric criteria and ductile fracture models for chip separation and chip segmentation. Chip separation was meant to occur when geometric separation of critical distance satisfies. The ductile fracture model was applied to crack growth during chip segmentation and was based on strain, strain rate, temperature and hydrostatic pressure. The critical equivalent plastic strain value (derived from impact compression test) was used for material failure due to localized adiabatic strain. Zhang et al. [211] developed an intra-granular damage model based on the crystallographic slip in grains and intergranular damage model formalized by zero thickness discrete cohesive elements for modelling chip segmentation of Ti-6Al-4V. Marusich and Ortiz [154] employed the hoop stress criterion of Erdogan and Shih to predict the crack path under brittle fracture conditions of materials. According to the adopted fracture criterion, the crack propagates at a certain angle when the maximum hoop stress reaches a critical maximum value. Ng et al. [190] adopted slip criteria to model the segmentation of chips of hardened steel. The catastrophic slip criterion can be explained as:

$$0 \leq -\frac{\partial T}{\partial \varepsilon^p} \times \frac{\partial T.dT}{\partial \tau.d\varepsilon} \leq 1, -----(16)$$

The catastrophic slip leading to segmentation occurs when the multiplication of two terms in eq. (16) equals 1.

Various researchers proposed the development of suitable deformation and damage models as chip separation criteria based on the experimentally observed cracking area [197, 212]. The material models employed in the modelling of

44

segmented chips include the Baummann-Chiesa-Johnson model [213], Johnson-Cook [155, 214], TANH law [155, 173, 215], and various other models [173, 216]. The most frequently adopted failure model for chip segmentation is Cockroft-Latham (C-L) damage model. Ceretti et al. [19, 193] employed the C-L model in combination with effective stress criteria to simulate continuous and segmented chip formation. The Cockroft-Latham model is defined as

$$C_i = \int_0^{\varepsilon_f} \bar{\sigma} \left(\frac{\sigma^{\mathrm{m}}}{\bar{\sigma}} \right) d\bar{\varepsilon}, - - - - - - (17)$$

where, C_i is the critical damage parameter adopted by uniaxial tension tests and ε_f is the fracture strain, $\bar{\sigma}$ and $\bar{\varepsilon}$ are the effective stress and effective strain and σ^m is the maximum stress value. In their model, when the values of the critical damage parameter C_i and effective stress reaches the maximum limit, chip separation occurs. The Cockroft-Latham damage model was used by many other researchers [60, 195, 217-220] for segmented chip formation.

The modelling of chip segmentation or breakage was also achieved through element deletion in the shear zone to simulate chip breakage. Ceretti et al. [19] adopted the chip segmentation model by element deletion at critical damage value. They claimed that by comparing the experimental data, chip segmentation for different materials under different conditions can be simulated using element deletion at critical damage criteria. Aurich and Bill [218] performed a 2D and 3D simulation of segmented chip formation using adiabatic shearing and crack formation and used the element deletion approach for chip formation.

The initial FE studies of discontinuous chip formation as a function of cutting conditions were conducted by Ueda et al. [221, 222] based on linear fracture

mechanics theory. They proposed a J-integral approach to model discontinuous chips by crack formation, as well as continuous chip formation [222]. When the J value exceeds critical value J_c, the crack propagation occurs in a brittle manner. If the J value doesn't exceed J_c, the simulation will continue and follow another criterion in which when the area of the plastic region S exceeds the critical value S_c, the primary deformation zone will be formed, and ductile continuous chips will be generated. Xi et al. [176] proposed the use of critical flow localization parameters as a function of material properties to predict the initiation of the shear band and chip breakage or chip serration. Lorentzon et al. [81] obtained discontinuous chips using plastic strain as fracture criterion at lower and higher cutting speeds. Obikawa et al. [179] performed a machining simulation of discontinuous chip formation based on geometrical and fracture strain criteria. They applied geometrical criteria for chip separation and fracture criteria for crack formation for discontinuous chips based on the following condition:

$$\dot{\bar{\varepsilon}}^p > \varepsilon_o$$

$$\varepsilon_o = \varepsilon_o - \alpha\frac{P}{\sigma} - \beta\frac{\dot{\bar{\varepsilon}}^p}{V_c} \leq 1, \qquad (18)$$

where, V_c is the cutting speed and α and β are material constants.

7. Friction criteria

7.1. Friction models

The friction between the workpiece and rake and flank faces of the tool governs chip formation behaviour and tool degradation in machining. The tool-chip contact area and friction parameters significantly influence temperature and stress distribution, cutting forces, and tool wears [16, 60, 66, 103, 223, 224]. Also cutting conditions and

46

parameters influence friction conditions [225, 226]. The correlation of frictional behaviour in experimental and simulation studies is highly dependent on the friction models used in cutting simulation [8, 68, 227]. Therefore, it is non-trivial to understand the frictional behaviour at the tool-chip interface as a function of tool and workpiece materials, geometry and cutting conditions.

Various friction models have been adopted and evaluated for performance in machining simulation studies. In these models, normal and shear stress distribution along the tool-chip interface provide the core understanding of frictional behaviour during cutting [226, 228-230]. Coulomb's law in its simplest form has extensively been adopted at the tool-chip interface in machining simulations in different FE machining models for a broad range of materials [56, 64, 82, 105, 190, 231] and described as

$$\tau_f = \mu \sigma_n - - - - - -(19)$$

Here, τ_f is frictional shear stress, μ is the friction coefficient and σ_n is normal stress acting on the surface.

At low cutting speed, Coulomb's friction can be used to assume rake and flank faces of the tool in contact with the chip and machined surface. However, in high-speed machining simulations, the exploitation of this basic model was criticized by many researchers [31, 60, 68]. Coulomb's model fails to address friction behaviour at high pressure and high sliding velocities as well as it provides frictional stresses larger than the shear yield strength of the material.

The constant shear friction model has also been adopted frequently by many researchers [10, 33, 232]. In the constant shear friction model, the frictional stress on the rake face is considered constant and is given by:

$$\tau_f = mk, \qquad (20)$$

where m is the shear friction factor and k is the shear flow stress of the workpiece material at tool-chip interfaces.

Fig. 15 shows the correlation of shear and normal stress in Coulomb and the constant shear model. In the sliding region, where both elastic and plastic deformation exist, the fictional shear stress becomes proportional to the normal stress [31] in Coulomb's model and remains constant in the constant shear model.
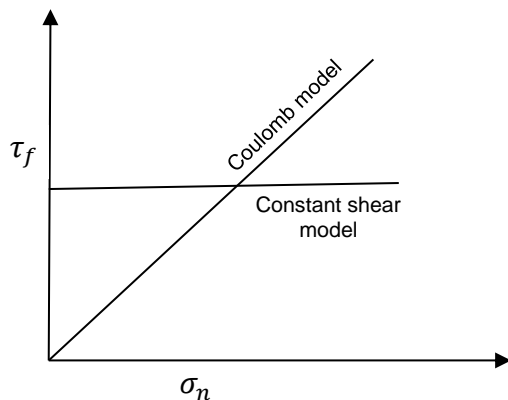

Fig. 15: Stress correlation in Coulomb and constant shear friction models

In metal cutting, sticking friction also develop in the sticking region at the tool-chip interface [4, 67, 224, 233] along with sliding friction. In the sticking region, the workpiece material sticks to the surface near the tool tip and shear flow occurs within chip ahead of stick material. Plastic friction dominates and frictional shear stress remains constant and equal to shear flow stress of the chip material at tool-chip interface. The extended Coulomb friction model adopted by Zorev [234] addresses the sticking and sliding friction behaviour along the tool-chip interface as a function of normal and shear stress distribution [235]. The model has been exploited successfully in FE machining studies for different FE models, material and cutting conditions [14, 15, 72, 184, 197, 225, 236] and is described as:

$$\tau_f = \begin{cases} \mu\sigma_n & when & \mu\sigma_n < \tau_c \ (Sliding) \\ \tau_c & when & \mu\sigma_n \geq \tau_c \ (Sticking) \end{cases} \quad ----(21)$$

where, τ_c, is the limiting shear flow stress.

Fig. 16 presents the distribution of stresses by Zorev's model along the sliding and sticking region. The normal stress decreases from a maximum at the tool cutting edges to zero at the end of tool-chip contact in the form of exponential decay. The shear stress remains constant from the tool cutting edge until the end of plastic contact or sticking region and then decreases exponentially to zero till the tool-chip contact boundary.
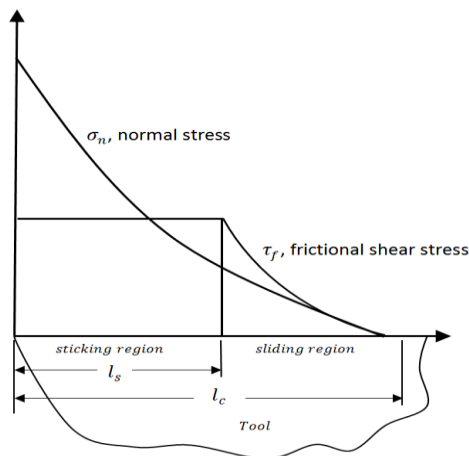

Fig.16: Stress distribution along tool-chip interface

In the sticking region, normal stress is high enough and frictional shear stress becomes equal to limiting shear flow stress. The performance of these stress distribution laws is dependent on the true calculation of tool-chip contact length (l_c) and sticking region length (l_s) [234, 237]. The tool-chip contact length can be measured experimentally as well as using a numerical approach [229, 230, 237, 238]. The length of the sticking and sliding zone can be estimated experimentally by analyzing different marks on the tool rake surface or by measuring stress distribution on the tool rake face during simulation.

Another friction model used in FE machining studies was developed by Usui and Shirakashi [233] based on the empirical stress characteristic equation. The model was applied in various simulation studies with good results [179, 239]. The frictional stress in the model is defined as

$$\tau_f = k\left[1 - e^{\left(\frac{-\mu\sigma_n}{k}\right)}\right] - - - - - -(22)$$

This model was later modified by Dirikolu et al. [165] to model the sliding friction behaviour at the tool-chip interface by multiplying k with m and refined the model with the following equation

$$\tau_f = mk\left[1 - e^{\left(\frac{-\mu\sigma_n}{mk}\right)^n}\right]^{1/n}, - - - - - - (23)$$

where, n is a constant and m follows the lubrication conditions $0 < m < 1$.

In many FE simulation studies of machining, different friction models were adopted in the sticking and sliding region. Ozel [5, 66] employed variable Coulomb friction, μ , constant shear friction factor, *m,* and contact pressure-dependent shear friction factor, *m(P),* to simulate 3D cutting simulations. Monaghan and MacGingley [73] characterize the tool-workpiece contact using combined Coulomb-Tresca friction law. Zhang and Bagchi [180] adopted a constant coefficient of friction in the sliding region and the shear strength of the workpiece in the sticking region. Shih and Yang [28] used constant friction value in the sticking region and variable value decreasing linearly from maximum to zero in the sliding region. Ozel [66, 67] employed constant and variable shear friction factors in the sticking region and constant and variable Coulomb's friction coefficient in the sliding region.

7.2. Friction coefficient

Friction behaviour at the tool-chip interface in various machining simulation studies was ignored or artificial friction coefficient values were used [29, 240]. This is due to the lack of real friction coefficient information for different cutting conditions and tool geometry. The friction coefficient values are commonly obtained from pin-on-disc methods and using Gradient friction coefficient and Mean friction coefficient methods [224]. Many tribological experimental and numerical studies have been developed to obtain an optimal friction coefficient of relevant materials at varying cutting conditions [29, 68, 189, 224, 240-243]. The most common way to predict the coefficient of friction μ in machining is from the measured experimental tangential (F_c) and thrust forces (F_t) using the following equation,

$$\mu = \frac{F_t + F_c tan\alpha}{F_c - F_t tan\alpha}, - - - - - - (24)$$

where, α is rake angle. Zemzemi et al. [241] developed an adhesive friction model based on local sliding velocity by conducting experimental and numerical tribology studies. They developed a new tribometer to characterize friction coefficient at relevant pressure and velocities involved at machining conditions. Sliding velocity was found to influence friction coefficient followed by pressure. The adhesion friction coefficient is defined as:

$$\mu_{adh} = A \times Ln(V_{ls}) + C, - - - - - -(25)$$

where μ_{adh} is the adhesive friction coefficient, V_{ls} is the average local sliding velocity. The parameters A and C are the model constants dependent on sliding velocity and macroscopic friction velocities.

The constant value of friction coefficient has been frequently adopted at the tool-chip interface which doesn't define real tool-chip contact behaviour during machining. More than 50% difference in the results of experimental and FE simulation studies has been found when using constant friction coefficient [68]. The variable friction coefficient can better predict the contact conditions at the tool-chip interface and offer a significant correlation of experimental and numerical studies. Arrazola et al. [68] developed a method to find a suitable variable Coulomb's friction coefficient based on non-continuous friction law and continuous friction law methods. In their study, the experimental and simulation results obtained using variable friction coefficient were found to improve accuracy close to 10%.

8. Material Constitutive models

Material constitutive models based on experimental, numerical, analytical and empirical studies have successfully been employed in numerical machining simulation studies. In order to numerically simulate the machining process, an accurate material model and solution technique need to be furnished. The plasticity and damage models are required to develop and assimilate in FEM codes. The plasticity models are essential to define material response behaviour during machining and in general, can be classified as rate-independent plasticity and viscoplasticity models. In rate-independent plasticity, the effect of strain rate is not considered in a stress-strain relationship whereas viscoplasticity is strain rate dependent plasticity. In machining, strain rate reaches in the range of 10^3–10^6 and for similar values of strain, stresses develop within the material are higher at higher strain rates. Therefore, viscoplastic models based on plastic strain rate can better predict realistic chip formation. Since during machining, the conversion of mechanical energy into heat energy contributes to the increase in cutting temperature, plasticity models which also include thermal

effects along with strain rate are essential for the true prediction of deformation behaviour in FE simulations. The constitutive models based on strain rate and temperature are known as thermo-viscoplastic models.

The FE machining simulations models employed in FE machining simulations can be categorized mainly into elastic-plastic [61, 169, 244] and rigid-plastic models [6, 178, 205, 207] with or without thermal and strain rate analyses [160, 164]. In rigid-plastic models, the elastic strains are ignored mainly due to the infinitesimal time interval for elastic deformation during high-speed machining. The rigid-plastic models are computationally less expensive than elastic-plastic models as later provide a detailed account of stresses and strains from incipient stage to steady-state. Fig. 17 shows an ideal stress-strain behaviour of the rigid-plastic and elastic-plastic model.
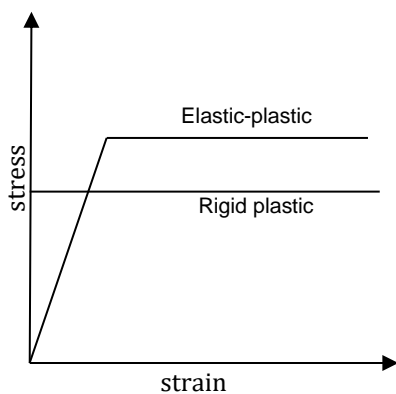
Fig. 17: Ideal behaviour of material models

The FE machining simulations with different constitutive models suggest that the material response behaviour is sensitive to the employed material model [58, 245]. The chip geometry, cutting forces and other solution variables are highly dependent on the constitutive material model [65, 86].

It is important to obtain material model parameters using the appropriate type of studies and at a relevant strain rate. There exists many parameters of a material model for a given workpiece material [56, 246, 247]. The material model parameters are

generally obtained through quasi-static and high dynamic (Split Hopkinson Pressure Bar, Taylor's impact, etc.) tensile, compression, torsion and shear tests at different temperature and strain rates [248-253]. Other methodologies include slot milling experiments [254], parametric optimization [213] and inverse modelling approach [104, 255] have also been used to determine the material model parameters. The rate-independent plasticity models are based on quasi-static experimental testing methods viz. tension, compression and torsion tests.

9. Tool wear Studies

One of the major contributions of FEM in machining simulations is to provide a platform to predict tool wear rate and its mechanism under a variety of machining conditions. Tool wear is a critical machining factor that has significant effects on principal output parameters including cutting forces, temperature, and surface finish. Tool wear mechanism and wear rate models are primarily based on empirical studies [90, 256-261]. The well-known model developed to estimate tool life based on machining conditions is Taylor's tool life equations and its modifications [262-264].

Tools that are frequently used in tool wear studies include coated and uncoated carbide tools, CBN, PCBN, cermet, and diamond tools [265, 266]. Depending on the type of tool, workpiece material and cutting conditions, the tool wear propagates under the influence of mechanical, chemical and thermo-mechanical contact [239].

There are multiple techniques developed to characterize the tool wear in FE cutting simulations. Research studies reveal that tool wear is dependent on cutting temperature, stresses, contact pressure and cutting velocity [35, 63, 267-269]. Monaghan and MacGinley [73, 270] studied tool wear in various coated and uncoated tungsten carbide and cemented carbide tools. They studied stress and temperature

distribution with different coatings in the PSZ, SDZ and coating boundaries and found the simulation results in good agreement with experimental results.

The FE simulation of tool wear studies requires the estimation of tool wear and modelling the same. Most of the FE studies integrated empirical or analytical tool wear models using user-defined subroutines incorporated in specific FEM packages [35, 265]. The general approach is to perform tool wear analysis via user-defined subroutine at steady-state chip conditions. The output solution variables (according to the wear model) are calculated at all nodes of the discretised tool which are in contact with the workpiece. The tool wears subroutine incorporates measured values of solution variables and calculate tool wear rate using the adopted empirical or analytical wear model. The geometry of the tool is then updated using calculated tool wear rate by a wear subroutine. Fig. 18 presents the basic steps to measure the tool wear in FE studies.
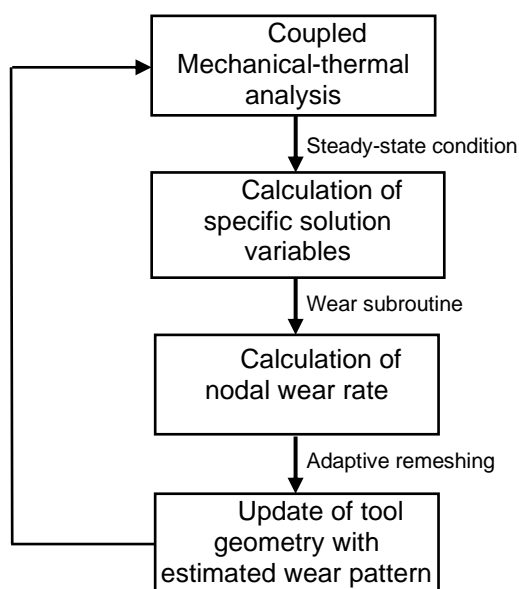

Fig.18: Basic methodology of tool wear measurement

Tool wear models implemented in FE-based tool wear simulation studies typically consider abrasion, adhesion and diffusion [69, 73, 90, 105-108, 271]. A pioneering numerical study in tool wear estimation was performed by Usui et al. [90] using adhesive wear based characteristic equation, predicting the temperature and stress distribution. The Usui's abrasive wear model has been frequently adopted in various other tool wear studies [3, 69, 265, 272]. The Usui model is described as

$$\dot{\omega} = F\sigma_n V_s exp\left(-\frac{L}{T}\right), - - - - (26)$$

where $\dot{\omega}$ is the wear rate and F and L are the tool and workpiece materials constants, respectively.

Attanasio et al. [107, 108, 273] performed 2D and 3D ALE based simulation studies of flank and crater tool wear of tungsten carbide based on diffusive wear mechanism. They adopted Takeyama and Murata (T-M) [258] tool wear model which is based on abrasive and diffusive wear. The model is described as,

$$\dot{\omega} = G(V, f) + Dexp\left(-\frac{E}{RT}\right), - - - (27)$$

where the term $G(V, f)$ represents abrasive wear contribution. The parameters V and f are the cutting speed and feed. The term E is the activation energy and R is the universal gas constant. They ignored the abrasive wear due to the high hardness of tungsten carbide as well as due to the reason that, in the T-M wear model at a temperature exceeding 700–800°C, the abrasive wear disappears and only diffusion takes place [274]. However, they found disagreement in the results of crater extension when using the T–M wear model. When using Usui's model, the simulation presents high error in crater depth and position compared to the experimental study [275]. In order to overcome the limitations of T-M and Usui wear models, they proposed a new

coupled abrasive-diffusive model by combining Usui and T-M wear model and performed tool wear study based on abrasive and diffusive wear mechanisms [106]. Molinari and Nouari [63, 267] proposed a diffusion wear model by considering the contact temperature as the main parameter in determining the diffusive wear rate. Zanger and Schulze [199, 269] performed tool wear studies and proposed a hybrid method of an experimental and numerical approach based on output data to calculate wear rate. They determined that Usui and T-M models can better predict wear rates using FEM analysis. Lorentzon and Jarvstrat [275] evaluated the Usui model and its two modified forms and T-M model using different frictional criteria. They concluded that Coulomb's friction model cannot accurately predict quantitative tool wear irrespective of the wear model used. Also, friction criteria significantly influence sliding velocity which consequently influences crater wear depth and location. Salvatore [276] presented tool crater wear modelling using the measurement of tool wear volume loss as a function of dissipated energy by friction. They adopted a predefined maximum energy approach at which elimination of nodes takes place when the dissipated energy reaches its maximum value.

The updation of tool geometry with wear pattern can be performed using element deletion method and nodal displacement methods [105, 199, 265]. The use of the nodal displacement method has been employed extensively. Yen et al [3, 272] performed a study on tool wear rate for uncoated carbide tools in cutting simulation of carbon steel. They used the Usui wear model [256] and evaluated tool wear at a discrete point in cutting time. Authors updated the rake and flank face geometry based on calculated wear using the Individual nodal movement method and also used average values of cutting variables. Xie et al. [105] also adopted the nodal movement method to model tool wear patterns. They adopted flank wear calculation subroutine

in the iteration model and implemented a predefined flank wear land width. The simulation continues in cycles until the predefined maximum flank wear land width is achieved. A similar approach of iteration model, maximum flank wear land width and nodal movement method is adopted by many researchers [199, 277]. When using the node movement method, the direction of nodal movement is in the direction of contact pressure at the relative node. The updation of tool geometry using the nodal displacement method results in mesh distortion. The mesh distortion was resolved using an adaptive remeshing procedure in which a new mesh is generated with updated geometry. Adaptive remeshing produce a tool wears pattern on the tool during the updating tool geometry stage [105, 106]. It has also been employed to smoothen the crater wear profile as well as mesh coarsening at the cutting edge [105].

Another approach utilized in characterizing the tool wear is by pre-defining the crater and flank wear in tool modelling and comparing the simulation results of new and predefined worn tools [3, 20, 266, 278, 279]. Different wear magnitudes and geometry can be modelled using this approach and the sensitivity of output variables is analyzed against various tool wear conditions.

10. Machining output variables

In order to understand the true response behaviour of the workpiece and tool during chip formation, it is necessary to determine the variation of output solution variables within chip formation zones as a function of input variables. The output solution variables obtained in FE simulations are node-based quantities (displacement, velocity, reaction force, etc.) or element-based quantities (stress, strain, etc.). In FE machining studies, various output parameters have been analyzed including yield stress, plastic strain, effective plastic stress and strain, temperature,

strain rate, hydrostatic stress, temperature, residual stress, cutting forces. The response of cutting forces and distribution of temperature and stresses as a function of input variables is briefly discussed in the following sections.

10.1. Cutting forces

Cutting forces have been frequently investigated to gain a pivotal understanding of the mechanics of chip formation and tool wear. High cutting forces can negatively affect the surface integrity of machined parts with tool wear. The cutting forces are generally analysed as a function of cutting force magnitude and its trend during cutting. The principal cutting forces components in machining simulations include tangential cutting force in the direction of cutting velocity, feed force in the direction of feed and thrust force normal to the velocity.

Tool geometry, friction parameters and shear angle are the three important parameters with a correlation that have a significant effect on cutting forces. In general principle, regardless of material type, a high coefficient of friction offers high frictional resistance and therefore high cutting forces. The FE studies [4, 94, 158, 184, 280] suggest that cutting forces increase with the decrease of rake angle and cutting edge radius. The studies also reveal that for the same tool geometry, when the coefficient of friction increases, the shear angle decreases.

Numerical simulation studies reveal that cutting forces are also affected by cutting speed. The magnitude of cutting force decreases with the increasing cutting speed [70]. However, this behaviour is highly dependent on the thermal conductivity of the tool and workpiece [72]. The studies also suggest that the machining response of reduction of cutting forces with increasing speed was found highly dependent on the feed rate [70]. The effect of material constitutive models in machining simulations was

59

investigated by many researchers [86, 155, 281]. The study revealed that cutting forces are the most influenced output variables when different constitutive material models are used using the same cutting conditions.

The cutting forces can be accurately estimated based on the frictional shear factor value. When using the smallest value of 0.1 in the cutting simulation, cutting forces can be predicted within a maximum of 4% error [60]. Tangential, thrust and feed forces can be highly influenced by the type of friction models used in cutting simulation [103]. When using constant and variable friction coefficients in two different simulations, the % difference between experimental and simulation feed forces are 50% and 10% respectively [68]. Arrazola and Ozel [67] compared Coulomb's friction and sticking-sliding friction using friction coefficient with finite sliding and shear stress limit. It was found a significant difference of 35% in thrust forces and an 11% difference in tangential forces. Haglund et al. [103] compared six different friction models including Coulomb, limited shear stress model and temperature-dependent friction coefficient model. Authors used constant and variable friction coefficients and in combination within the sticking and sliding region. The findings suggest the significant influence of friction models on tangential and feed forces.

10.2. Cutting temperature

During machining, the high cutting temperature may lead to desirable or undesirable effects depending on the tool and workpiece material and cutting conditions. It could ease machining by material softening or could result in tool wear and thermal expansion and undesirable residual stresses consequently affecting machining performance. Although there exist experimental and analytical methods to record temperature [172, 282-285], it is difficult to monitor the exact cutting

temperature locally as well as its distribution at the tool-chip interface. FEM is regarded as a highly valuable tool in the prediction of cutting temperature during machining and its distribution [232]. The cutting temperature in FE machining simulations is usually analyzed to estimate chip and machined surface behaviour, variation in mechanical properties and tool wear.

One of the critical factors to consider in FE machining simulations is temperature distribution in different deformation zones and in cutting tools [167, 282]. The conversion of mechanical energy into heat energy at the tool-workpiece interface during chip formation inspires higher cutting temperature. In Primary Shear Zone (PSZ), heat is produced during chip formation owing to plastic deformation. Dependent on the chip geometry, heat in Secondary Deformation Zone (SDZ) is generated due to plastic deformation and friction between chip and tool rake surface along the contact length and also contribute to cutting temperature. The heat produces in the Tertiary Deformation Zone (TDZ) is due to the friction between the tool flank face and machined surface. The heat generated in TDZ is initially in small magnitude and start contributing to cutting temperature with the progression of tool wear. Fig. 19 presents general heat generation and transfer zones.
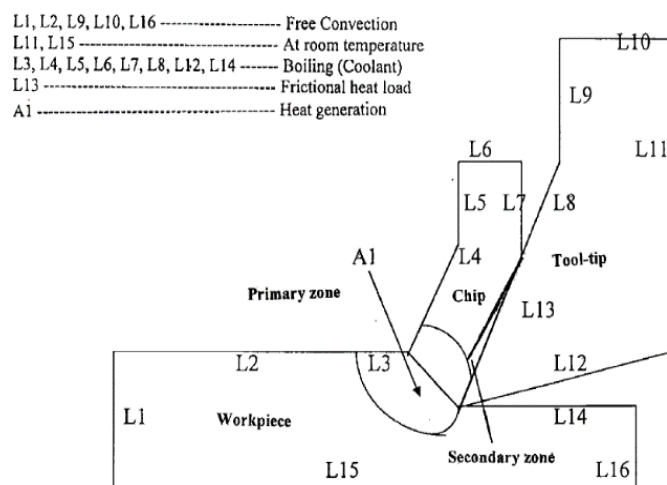

Fig.19: Thermal activity during chip formation [54]

61

The thermal analyses in FE cutting simulations are based on heat generation by plastic deformation and friction. The conduction within workpiece and tool as well as convection effects has also been considered in cutting simulations [6, 202, 238]. The majority of thermo-mechanical numerical studies [6, 7, 72, 202, 204, 286] adopted global thermal conduction or heat flow equation at the steady-state condition which can be expressed as

$$\chi\left(\frac{\partial^2 T}{\partial x^2} + \frac{\partial^2 T}{\partial y^2}\right) + \dot{Q} = \rho C_p\left(u_x \frac{\partial T}{\partial x} + u_y \frac{\partial T}{\partial y}\right), - - - - -(28)$$

where, χ, is the thermal conductivity, $\dot{Q}$ is the rate of heat flux of specific volume, and C_p is the specific heat of the material. The parameters u_x and u_y are the material flow velocity components in the x and y direction respectively.

The frictional heat, q_f generated due to tool and workpiece contact during chip formation is given by

$$q_f = \frac{\tau V_s}{M}, - - - - (29)$$

where, M is the mechanical equivalent of heat. The heat flux q_v due to convection between tool or workpiece and environment is given by

$$q_v = h_c(T_g - T_{room}), - - - - (30)$$

where, h_c is the heat transfer coefficient of convection and T_g is the temperature of the tool or workpiece.

The majority of FE machining simulation work is based on the study and evaluation of temperature distribution at steady-state conditions. A pioneering study of temperature distribution analysis was done by Tay et al. [287], in which the authors

62

studied the temperature gradient across the shear plane for characterization of material properties and work-hardening rate. The temperature of the chip surface is generally obtained as average temperature by adding the temperature of all the nodes of the chip surface divided by the number of nodes. Numerical studies suggest that the maximum heat generation takes place in the PSZ and SDZ caused by plastic deformation and sliding and sticking friction [7, 11, 59, 72, 284]. The temperature in SDZ was found higher than the PSZ [70, 204] for a wide range of metals.

The temperature distribution at the rake and flank faces of the tool has also been studied [6, 7, 72, 266, 284]. The average temperature is found to rise with an increase in the cutting velocity [6, 59, 232] and tool rake angle. The increase of the coefficient of friction results in frictional resistance in the SDZ which leads to an increase in cutting temperature at the tool-chip interface. The temperature distribution remains non-uniform as a function of chip geometry along the rake face and maximum temperature occurs just above the cutting edge. The temperature on the rake face was observed much higher than the flank face of the tool.

The effect of machining input variables on cutting temperature including cutting speed, feed, cutting depth, and tool material and geometry have largely been investigated [6, 7, 63, 72, 202, 268, 288, 289]. The thermal conductivity of the tool and workpiece materials contributes significantly to the cutting temperature. The cutting tool with higher thermal conductivity offers better performance when cutting lower-thermal conductivity workpiece material than cutting a workpiece with higher thermal conductivity [286].

10.3. Cutting stresses

The stress distribution on the tool-chip interface in FE machining studies has widely been studied [97, 234, 235]. The stress distribution models are based on data obtained using different experimental methods including photoelastic and split tool methods [229, 230, 290, 291]. Before the surge in the use of commercial FE packages, individual stress components were measured to record deformation conditions. von Mises is the most frequently studied yielding criteria in FE cutting simulations [150, 200, 292] using commercial software. According to the von Mises yield criterion, initial yielding occurs when the deviatoric stress invariant acquires a critical value. The von Mises criterion in terms of principle stresses is described as:

$$(\sigma_1 - \sigma_2)^2 + (\sigma_2 - \sigma_3)^2 + (\sigma_3 - \sigma_1)^2 = 2\sigma_Y^2, ---(31)$$

where, σ_1, σ_2 and σ_3 are principal stresses and σ_Y is the yield stress of the material.

Research studies suggest that in machining, the magnitude of von Mises stresses is higher near the tooltip in PSZ compared to SDZ and TDZ [70, 150, 151, 204]. The intensity of the stresses varies along with the tool-chip interface as a function of tool rake angle and cutting edge.

The stress distribution on the machined surface in terms of residual stresses has also been the topic of interest. Machining is a process that involves plastic deformation, heat generation and many other mechanical, chemical and thermal effects. After machining, some stresses remain within the final machined surface which influences the form accuracy and surface finish of the material. These stresses are called residual stresses which are the distributed stresses on and under the machined surface after machining.

In FE machining simulations, residual stresses are generally recognized as tensile stresses and compressive stresses along cutting direction and perpendicular to cutting direction [4, 8, 28, 150, 202, 293]. When measuring residual stress, the elements at the final machined surface should be chosen at points sufficiently away from the tool edge and from the boundary conditions to reduce the influence of both factors. High mesh density in the chip formation zone is required to improve the prediction of residual stresses in machining simulations [84].

Research studies suggest that residual stresses in the machined surface increase with the decrease of rake angle and an increase of cutting-edge radius and tool wear [244, 294-296]. The other factors which significantly influence residual stresses are: material hardness [297], undeformed chip thickness [244, 296, 298], cutting velocity and feed rate [59, 150, 151], frictional resistance [4, 11, 202, 293, 299-301], sequential cutting [201] and material models [281]. One of the main undesired effects of these parameters is the mechanical deformation of the machined surface which leads to the generation of high tensile and compressive residual stresses [302]. In residual stress studies, the material flowing under the cutting edge towards the flank side is attributed to the ploughing of material. The thickness of ploughing depth largely influences the temperature and residual stresses and, therefore, surface integrity of the machined surface [293, 301, 303, 304].

11.   Summary and Conclusion

This paper systematically and comprehensively reviews the stat-of-the-art techniques and methodologies used in the development of FE modelling of tribology of metals. The mesh-based and meshless approaches employed in plastic deformation of metals are discussed. Different friction criteria, constitutive models and

tool wear studies are discussed. Based on this review, the following conclusions can be made:

- Meshless methods have great potential to perform realistic material separation criterion and wear studies without suffering mesh distortion issues. However, FE software containing meshless methods does not allow full thermo-mechanical analysis using particle methods. Also, there is a limitation of the contact definition of two meshless surfaces. Specialized machining FE codes do not feature meshless methods.

- Material separation criteria are the most crucial aspect of tribological simulations as it influences the results of all the output variables. The accuracy of geometrical separation criterion and physical separation criterion is highly dependent on the selection of the critical value of the parameter. Geometrical separation criteria suffer the limitation of tool geometry including geometry of the cutter. The criteria cannot be accurately used for negative rake angle and higher cutting-edge radius. In most of the previously reported simulation studies, the values of critical parameters of these criteria were mainly obtained without any sophisticated designed rules. For a given workpiece material, the critical value may vary as a function of FE model type, the scale of cutting, conditions of cutting, tool geometry and various other factors. Large experimental studies, as well as extensive trial and error simulation studies, are required to validate the true threshold geometric or physical values.

- There is a wide range of material model parameters that exist for a given material with a good difference in magnitude. These parameters provide the basis of deformation behaviour during chip formation and maintaining

steady-state conditions. There is a need to develop a sophisticated methodology to obtain realistic material model parameters.

- Most wear studies are based on indirect methods of calculation of output solution variables based on mathematical wear models. Although this strategy provides good observation of tool wear, the method is highly dependent on a true prediction of tool-chip interface conditions including friction criteria and temperature and stress distribution.

- While considering thermal analysis, the conduction through the tool as well as convection to the environment has been largely ignored during most of the cutting simulation studies.

Acknowledgement

References

1.   Arrazola, P.J., et al., *Recent advances in modelling of metal machining processes.* CIRP Annals - Manufacturing Technology, 2013. **62**(2): p. 695-718.
2.   Jawahir, I.S., et al., *Surface integrity in material removal processes: Recent advances.* CIRP Annals - Manufacturing Technology, 2011. **60**(2): p. 603-626.
3.   Yen, Y.-C., et al., *Estimation of tool wear in orthogonal cutting using the finite element analysis.* Journal of Materials Processing Technology, 2004. **146**(1): p. 82-91.
4.   Shih, A.J., *Finite Element Analysis of the Rake Angle Effects in orthogonal metal cutting.* International Journal of Mechanical Sciences, 1996. **38**(1): p. 1-17.
5.   Özel, T., *Computational modelling of 3D turning: Influence of edge micro-geometry on forces, stresses, friction and tool wear in PcBN tooling.* Journal of Materials Processing Technology, 2009. **209**(11): p. 5167-5177.
6.   Moriwaki, T., N. Sugimura, and S. Luan, *Combined Stress, Material Flow and Heat Analysis of Orthogonal Micromachining of Copper.* CIRP Annals - Manufacturing Technology, 1993. **42**(1): p. 75-78.
7.   Muraka, P.D., G. Barrow, and S. Hinduja, *Influence of the process variables on the temperature distribution in orthogonal machining using the finite element method.* International Journal of Mechanical Sciences, 1979. **21**(8): p. 445-456.
8.   Arrazola, P.J. and T. Özel, *Numerical modelling of 3D hard turning using arbitrary Lagrangian Eulerian finite element method.* Mechanical Engineering, 2008. **3**(3): p. 238-249.
9.   Davoudinejad, A., et al., *Finite Element Simulation and Validation of Chip Formation and Cutting Forces in Dry and Cryogenic Cutting of Ti–6Al–4V.* Procedia Manufacturing, 2015. **1**: p. 728-739.
10.   Pu, Z., et al., *Finite Element Simulation of Residual Stresses in Cryogenic Machining of AZ31B Mg Alloy.* Procedia CIRP, 2014. **13**: p. 282-287.
11.   Mohammadpour, M., M.R. Razfar, and R. Jalili Saffar, *Numerical investigating the effect of machining parameters on residual stresses in orthogonal cutting.* Simulation Modelling Practice and Theory, 2010. **18**(3): p. 378-389.
12.   Ali, M.H., et al., *FEM to predict the effect of feed rate on surface roughness with cutting force during face milling of titanium alloy.* HBRC Journal, 2013. **9**(3): p. 263-269.
13.   Korkut, I. and M.A. Donertas, *The influence of feed rate and cutting speed on the cutting forces, surface roughness and tool–chip contact length during face milling.* Materials & Design, 2007. **28**(1): p. 308-312.
14.   Rotella, G. and D. Umbrello, *Finite element modeling of microstructural changes in dry and cryogenic cutting of Ti6Al4V alloy.* CIRP Annals - Manufacturing Technology, 2014. **63**(1): p. 69-72.

68

15. Shet, C., X. Deng, and A. E. Bayoumi, *Finite element simulation of high-pressure water-jet assisted metal cutting.* International Journal of Mechanical Sciences, 2003. **45**(6-7): p. 1201-1228.

16. Banerjee, N. and A. Sharma, *Identification of a friction model for minimum quantity lubrication machining.* Journal of Cleaner Production, 2014. **83**: p. 437-443.

17. Abolfazl Zahedi, S., et al., *FE/SPH modelling of orthogonal micro-machining of f.c.c. single crystal.* Computational Materials Science, 2013. **78**: p. 104-109.

18. Demiral, M., A. Roy, and V.V. Silberschmidt, *Strain-gradient crystal-plasticity modelling of micro-cutting of b.c.c. single crystal.* Meccanica, 2015. **51**(2): p. 371-381.

19. E. Ceretti, p.F., W. T. Wu , T. Altan, *Application of 2D FEM to chip formation in orthogonal cutting.* Journal of Materials Processing Technology, 1996. **59**: p. 169-180.

20. Chen, L., T.I. El-Wardany, and W.C. Harris, *Modelling the Effects of Flank Wear Land and Chip Formation on Residual Stresses.* CIRP Annals - Manufacturing Technology, 2004. **53**(1): p. 95-98.

21. Carroll, J.T. and J.S. Strenkowski, *Finite Element Models of Orthogonal Cutting with Application to Single Point Diamond Turning.* International Journal of Mechanical Sciences, 1988. **30**(12): p. 899-920.

22. Lin, Z.C. and W.C. Pan, *A thermoelastic-plastic large deformation model for orthogonal cutting with tool flank wear - Part 1: Computational Procedures.* International Journal of Mechanical Sciences, 1993. **35**(10): p. 829-840.

23. Usui E, S.T., *Mechanics of machining- From descriptive to predictive theory, on the art of cutting metals-75 years later a tribute to F W Taylor.* ADME PED, 1982. **7**: p. 13-30.

24. Zhang, L., *On the seperation criteria in the simulation of orthogonal metal cutting using the finite element method.* Journal of Materials Processing Technology, 1999. **89-90**: p. 273-278.

25. Movahhedy, M., M.S. Gadala, and Y. Altintas, *Simulation of the orthogonal metal cutting process using an arbitrary Lagrangian–Eulerian finite-element method.* Journal of Materials Processing Technology, 2000. **103**(2): p. 267-275.

26. Bäker, M., J. Rösler, and C. Siemers, *A finite element model of high speed metal cutting with adiabatic shearing.* Computers & Structures, 2002. **80**(5-6): p. 495-513.

27. Sekhon, G.S. and J.L. Chenot, *Numerical Simulation of Continuous Chip Formation during Non-Steady Orthogonal Cutting.* Engineering Computations, 1993. **10**(1): p. 31-48.

28. Shih, A.J. and H.T.Y. Yang, *Experimental and finite element predictions of residual stresses due to orthogonal metal cutting.* International Journal for Numerical Methods in Engineering, 1993. **36**(9): p. 1487-1507.

29. Zanger, F., N. Boev, and V. Schulze, *Novel Approach for 3D Simulation of a Cutting Process with Adaptive Remeshing Technique.* Procedia CIRP, 2015. **31**: p. 88-93.

30. Davim, J.P., *Machining of hard materials.* 2011, London: Springer.

31. Quiza, R., O. López-Armas, and J.P. Davim, *Finite Element in Manufacturing Processes.* 2012: p. 13-37.

69

32.   Mackerle, J., *Finite-element analysis and simulation of machining: a bibliography (1976–1996).* Journal of Materials Processing Technology, 1998. **86**(1-3): p. 17-44.
33.   Ceretti, E., et al., *Turning Simulations Using a Tree-Dimensional FEM Code.* Journal of Materials Processing Technology, 2000. **98**: p. 99-103.
34.   Ducobu, F., E. Rivière-Lorphèvre, and E. Filippi, *On the introduction of adaptive mass scaling in a finite element model of Ti6Al4V orthogonal cutting.* Simulation Modelling Practice and Theory, 2015. **53**: p. 1-14.
35.   Guediche, M., et al., *A New Procedure to Increase the Orthogonal Cutting Machining Time Simulated.* Procedia CIRP, 2015. **31**: p. 299-303.
36.   Bİrcan, D.A., *Investigation of Cutting Parameters of Drilling Ti6Al4V Using Finite Element Analysis.* International journal of natural and engineering sciences, 2015. **9**(2): p. 25-31.
37.   Chen, W.C., *Effect of the cross-sectional shape design of a drill body on drill temperature distributions.* International Communications in Heat and Mass Transfer, 1996. **23**(3): p. 355-366.
38.   Fallis, A.G., *Finite element analysis of hastelloy C-22Hs in end milling.* Journal of Mechanical engineering and sciences, 2011. **1**: p. 37-46.
39.   Adetoro, M.B. and P.H. Wen. *FEM Evaluation of Mechanistic Cutting Force Coefficients Using ALE Formulation.*
40.   Hu, F. and D. Li, *Modelling and Simulation of Milling Forces Using an Arbitrary Lagrangian–Eulerian Finite Element Method and Support Vector Regression.* Journal of Optimization Theory and Applications, 2011. **153**(2): p. 461-484.
41.   Man, X., et al., *Validation of Finite Element Cutting Force Prediction for End Milling.* Procedia CIRP, 2012. **1**: p. 663-668.
42.   Gururaj Bolar, S.N.J., *Three-dimensional numerical modeling, simulation and experimental validation of milling of a thin-wall component.* Proceedings of the Institution of Mechanical Engineers, Part B: Journal of Engineering Manufacture, 2014. **231**(5): p. 792-804.
43.   Holtermann, R., et al., *Towards the simulation of grinding processes - a thermoplastic single grain approach.* Pamm, 2011. **11**(1): p. 385-386.
44.   Fuh, K.-h. and J.-s. Huang, *Thermal analysis of creep-feed grinding.* Journal of Materials Processing Technology, 1994. **43**: p. 109-124.
45.   Aspinwall, D.K. and S.L. Soo, *Developments in modelling of metal cutting processes.* Proceedings of the Institution of Mechanical Engineers, Part L: Journal of Materials: Design and Applications, 2007. **221**(4): p. 197-211.
46.   Nirmal K, G.G.S.G., *Emergence of machine learning in the development of high entropy alloy and their prospects in advanced engineering applications.* Emergent Materials, 2021. **4**: p. 1635-1648.
47.   Yuhang Pan, P.Z., Ying Yan, Anupam Agarwar, Yonghao Wang, Dongmin Guo, Saurav Goel, *New insights into the methods for predicting ground surface roughness in the age of digitalisation.* Precision Engineering, 2021. **67**: p. 393-418.
48.   Dragos Axinte, Y.G., Zhirong Liao, Albert J.Shih, Rachid MSaoubi, Naohiko Sugita, *Machining of biocompatible materials-Recent advances.* CIRP Annals - Manufacturing Technology, 2019. **68**: p. 629-652.
49.   Zhirong Liao, D.A.A., *On Chip fomration mechanism in orthogonal cutting of bone.* International journal of machine tools and manufacture, 2016. **102**: p. 41-55.

50. Strenkowski, J.S. and J.T. Carroll, *A Finite Element Model of Orthogonal Metal Cutting.* Journal of Engineering for Industry, 1985. **107**(4): p. 349.

51. Engelmann, B.E. and J.O. Hallquist, *NIKE2D: A non linear implicit two dimensional finite element code for solid mechanics*, in *User manual*, L.L.N. Laboratory, Editor. 1991.

52. Sadat, A.B., M.Y. Reddy, and B.P. Wang, *Plastic-Deformation Analysis in Machining of Inconel-718 Nickel-Base Superalloy Using Both Experimental and Numerical-Methods.* International Journal of Mechanical Sciences, 1991. **33**(10): p. 829-842.

53. Chen, G., et al., *Finite element simulation of high-speed machining of titanium alloy (Ti–6Al–4V) based on ductile failure model.* The International Journal of Advanced Manufacturing Technology, 2011. **56**(9-12): p. 1027-1038.

54. Haddag, B., et al., *Finite element formulation effect in three-dimensional modeling of a chip formation during machining.* International Journal of Material Forming, 2010. **3**(S1): p. 527-530.

55. Gao, C.Y., *FE realization of thermo-visco-plastic constitutive models using VUMAT in ABAQUS/Explicit Program.* Computational Mechanics ISCM2007, 2007: p. 623-628.

56. Ozel, T., et al., *3d Finite Element Modelling of Chip Formation Process for Machining Inconel 718: Comparison of Fe Software Predictions.* Machining Science and Technology, 2011. **15**(1): p. 21-46.

57. Limido, J., et al., *SPH method applied to high speed cutting modelling.* International Journal of Mechanical Sciences, 2007. **49**(7): p. 898-908.

58. Schwer, L., *Optional Strain-Rate Forms for the Johnson Cook Constitutive Model and the Role of the Parameter Epsilon _ 01.* 6th European LS_DYNA Users' Conference, 2007: p. 1-17.

59. Majumdar, P., R. Jayaramachandran, and S. Ganesan, *Finite element analysis of temperature rise in metal cutting processes.* Applied Thermal Engineering, 2005. **25**(14-15): p. 2152-2168.

60. Bil, H., S.E. Kılıç, and A.E. Tekkaya, *A comparison of orthogonal cutting data from experiments with three different finite element models.* International Journal of Machine Tools and Manufacture, 2004. **44**(9): p. 933-944.

61. Branis, A.S. and D.E. Manolakos, *Finite element simulation of chip formation in orthogonal metal cutting.* Journal of Materials Processing Technology, 2001. **110**: p. 19-27.

62. Corina CONSTANTIN, S.-M.C., George CONSTANTIN, and E. STRĂJESCU, *FEM tools for cutting process modelling and simulation.* University Politehnica Of Bucharest Scientific Bulletin-Series A-Applied Mathematics And Physics, 2012. **74**(4).

63. Nouari, M. and A. Molinari, *Experimental verification of a diffusion tool wear model using a 42CrMo4 steel with an uncoated cemented tungsten carbide at various cutting speeds.* Wear, 2005. **259**(7-12): p. 1151-1159.

64. Grzesik, W., M. Bartoszuk, and P. Nieslony, *Finite element modelling of temperature distribution in the cutting zone in turning processes with differently coated tools.* Journal of Materials Processing Technology, 2005. **164-165**: p. 1204-1211.

65. Klocke, F., H.W. Raedt, and S. Hoppe, *2d-Fem Simulation of the Orthogonal High Speed Cutting Process.* Machining Science and Technology, 2001. **5**(3): p. 323-340.

66.   Özel, T., *The influence of friction models on finite element simulations of machining.* International Journal of Machine Tools and Manufacture, 2006. **46**(5): p. 518-530.

67.   Arrazola, P.J. and T.r. Özel, *Investigations on the effects of friction modeling in finite element simulation of machining.* International Journal of Mechanical Sciences, 2010. **52**(1): p. 31-42.

68.   Arrazola, P.J., D. Ugarte, and X. Domínguez, *A new approach for the friction identification during machining through the use of finite element modeling.* International Journal of Machine Tools and Manufacture, 2008. **48**(2): p. 173-183.

69.   Zhang, B., et al., *Finite elementt simulation and analysis on wear of mechanical graver for diffraction grating.* Journal of Theoretical and Applied Information Technology, 2012. **46**(1): p. 289-293.

70.   Seshadri, R., et al., *Finite Element Simulation of the Orthogonal Machining Process with Al 2024 T351 Aerospace Alloy.* Procedia Engineering, 2013. **64**: p. 1454-1463.

71.   Gavrus, A., P. Caestecker, and E. Ragneau, *Finite Element Analysis of the Influence of the Material Constitutive Law Formulation on the Chip Formation Process during a High Speed Metal Cutting.* Proceedings of the Asme 11th Biennial Conference on Engineering Systems Design and Analysis, 2012, Vol 1, 2012: p. 543-551.

72.   Ng, E.G., et al., *Modelling of temperature and forces when orthogonally machining hardened steel.* International Journal of Machine Tools and Manufacture, 1999. **39**: p. 885-903.

73.   Monaghan, J. and T. MacGinley, *Modelling the Orthogonal Machining Process Using Coated carbide cutting tools.* Computational Materials Science, 1999. **16**: p. 275-284.

74.   Arrazola, P.J., *Finite element modeling and simulation*, in *Machining of hard materials*, J.P. Davim, Editor. 2010. p. 143-172.

75.   Gardner, J.D., A. Vijayaraghavan, and D.A. Dornfeld, *Comparative Study of Finite Element Simulation Software.* 2005.

76.   Thirdwave, *Third wave advantedge workshop manual*, T.w. systems, Editor. 2015.

77.   Markopoulos, A.P., *Application of FEM in metal cutting*, in *Finite element method in machining process*, J.P. Davim, Editor. 2013, Springer.

78.   Fluhrer, J., *DEFROM Design Environment for forming*, in *USer manual*, S.F.T. Corporation, Editor. 2014.

79.   Karajan, N., et al. *Particle methods in LS-DYNA.* 2014.

80.   Xu, J. and J. Wang. *Interaction Methods for the SPH Parts (Multiphase flows, solid bodies), in LS-DYNA.* 2014.

81.   Lorentzon, J., N. Järvstråt, and B.L. Josefson, *Modelling chip formation of alloy 718.* Journal of Materials Processing Technology, 2009. **209**(10): p. 4645-4653.

82.   Amrita Priyadarshinin, S.K.P., Arun K. Samantaray, *Finite Element modeling of chip formation in orthogonal machining*, in *Statistical and computational techniques in manufacturing*, J.P. Davim, Editor. 2012: London.

83.   Komvopoulos, K. and S.A. Erpenbeck, *Finite Element Modeling of Orthogonal Metal Cutting.* Journal of Engineering for Industry, 1991. **113**(3): p. 253.

84.   Shih, A.J., *Finite Element Simulation of Orthogonal Metal Cutting.* Journal of Manufacturing Science and Engineering, 1995. **117**(1): p. 84-84.

72

85. Shih, A.J.M., S. Chandrasekar, and H.T.Y. Yang, *Finite element simulation of metal cutting process with strain-rate and temperature effects.* ASME PED, 1990. **43**: p. 11-24.

86. Ducobu, F., E. Rivière-Lorphèvre, and E. Filippi, *Material constitutive model and chip separation criterion influence on the modeling of Ti6Al4V machining with experimental validation in strictly orthogonal cutting condition.* International Journal of Mechanical Sciences, 2016. **107**: p. 136-149.

87. Mahnama, M. and M.R. Movahhedy, *Application of FEM simulation of chip formation to stability analysis in orthogonal cutting process.* Journal of Manufacturing Processes, 2012. **14**(3): p. 188-194.

88. Klamecki, B.E., *Incipient chip formation in metal cutting a three dimension finite element analysis :PhD thesis.* University of Illinois, 1973.

89. Mir, A., *The investigation of influence of tool wear on ductile to brittle transition in single point diamond turning of silicon.* 2017, University of Strathclyde.

90. Usui, E., T. Shirakashi, and T. Kitagawa, *Analytical Prediction of Three Dimensional Cutting Process—Part 3: Cutting Temperature and Crater Wear of Carbide Tool.* Journal of Engineering for Industry, 1978. **100**(2): p. 236.

91. Usui, E., A. Hirota, and M. Masuko, *Analytical prediction of three dimensional cutting process. part 1. Basic cutting model and energy approach.* Trans ASME-J Eng Ind, 1978. **100**: p. 222-228.

92. Usui, E. and A. Hirota, *Analytical prediction of three dimensional cutting process. part 2. chip formation and cutting force with conventional single-point tool.* Trans ASME-J Eng Ind, 1978. **100**: p. 229-235.

93. Strenkowski, J.S. and J.T. Carroll, III. *An orthogonal metal cutting model based on an Eulerian finite element method,Manufacturing Processes, Machines and Systems.* 1986.

94. Strenkowski, J.S., A.J. Shih, and J.C. Lin, *An analytical finite element model for predicting three-dimensional tool forces and chip flow.* International Journal of Machine Tools and Manufacture, 2002. **42**(6): p. 723-731.

95. Strenkowski, J.S. and K.-J. Moon, *Finite Element Prediction of Chip Geometry and Tool/Workpiece Temperature Distributions in Orthogonal Metal Cutting.* Journal of Engineering for Industry, 1990. **112**(4): p. 313.

96. Athavale, S.M., J.S. Strenkowski, and N. Carolina, *Material Damage-Based Model for Predicting Chip-Breakability.* Journal of Manufacturing Science and Engineering, 1997. **119**(NOVEMBER): p. 675-680.

97. Puls, H., F. Klocke, and D. Lung, *Experimental investigation on friction under metal cutting conditions.* Wear, 2014. **310**(1-2): p. 63-71.

98. Wang, C.C., *Finite Element Simulation for Forging Process Using Euler's Fixed Meshing Method.* Materials Science Forum, 2008. **575-578**: p. 1139-1144.

99. Donea, J., et al., *Arbitrary Lagrangian-Eulerian Methods.* 2004, John Wiley and Sons Ltd. p. 1-25.

100. Movahhedy, M.R., Y. Altintas, and M.S. Gadala, *Numerical Analysis of Metal Cutting With Chamfered and Blunt Tools.* Journal of Manufacturing Science and Engineering, 2002. **124**(2): p. 178.

101. Olovsson, L., L. Nilsson, and K. Simonsson, *ALE formulation for the solution of two-dimensional metal cutting problems.* Computers and Structures, 1999. **72**(4): p. 497-507.

102. Li, L., Y. Ding, and V. Engineering. *Finite element modeling method of chip formation based on ale approach.* 2010. ASME Digital Collection.

103. Haglund, A.J., H.A. Kishawy, and R.J. Rogers, *An exploration of friction models for the chip–tool interface using an Arbitrary Lagrangian–Eulerian finite element model.* Wear, 2008. **265**(3-4): p. 452-460.
104. Agmell, M., A. Ahadi, and J.-E. Ståhl, *Identification of plasticity constants from orthogonal cutting and inverse analysis.* Mechanics of Materials, 2014. **77**: p. 43-51.
105. Xie, L.J., et al., *2D FEM estimate of tool wear in turning operation.* Wear, 2005. **258**(10): p. 1479-1490.
106. Attanasio, A., et al., *Investigation and FEM-based simulation of tool wear in turning operations with uncoated carbide tools.* Wear, 2010. **269**(5-6): p. 344-350.
107. Attanasio, A., et al., *3D finite element analysis of tool wear in machining.* CIRP Annals - Manufacturing Technology, 2008. **57**(1): p. 61-64.
108. A. Attanasio, E.C., C. Giardini, L. Filice, D. Umbrello, *Criterion to evaluate diffusive wear in 3D simulations when turning AISI 1045 steel.* International Journal of Material Forming, 2008. **1**: p. 495-498.
109. Gingold, R.A. and J.J. Monaghan, *Smoothed particle hdyrodynamics: theory and application to non-spherical stars.* Mon. Not. R.astr. Soc., 1977. **181**: p. 375-389.
110. Ambati, R., et al., *Application of material point methods for cutting process simulations.* Computational Materials Science, 2012. **57**: p. 102-110.
111. Idelsohn, S.R., E. Oñate, and F.D. Pin, *The particle finite element method: a powerful tool to solve incompressible flows with free-surfaces and breaking waves.* International Journal for Numerical Methods in Engineering, 2004. **61**(7): p. 964-989.
112. OÑAte, E., et al., *the Particle Finite Element Method — an Overview.* International Journal of Computational Methods, 2004. **01**(02): p. 267-307.
113. Onate, E. and R. Owen, *Particle-based methods Fundamentals and applications.* Vol. 25. 2011: Springer.
114. Idelsohn, S.R., et al., *The meshless finite element method.* International Journal for Numerical Methods in Engineering, 2003. **58**(6): p. 893-912.
115. Oñate, E., et al., *Advances in the particle finite element method for the analysis of fluid–multibody interaction and bed erosion in free surface flows.* Computer Methods in Applied Mechanics and Engineering, 2008. **197**(19-20): p. 1777-1800.
116. Oñate, E., M.A. Celigueta, and S.R. Idelsohn, *Modeling bed erosion in free surface flows by the particle finite element method.* Acta Geotechnica, 2006. **1**(4): p. 237-252.
117. E. Oñate , R.O., *Particle finite element method in solid mechanics problem*, in *computational plasticity.* 2007, Springer: Dordrecht.
118. Carbonell, J.M., E. Oñate, and B. Suárez, *Modelling of tunnelling processes and rock cutting tool wear with the particle finite element method.* Computational Mechanics, 2013. **52**(3): p. 607-629.
119. Sabel, M., C. Sator, and R. Müller, *Particle Finite Element Analysis of Cutting Processes.* Pamm, 2014. **14**(1): p. 259-260.
120. Sabel, M., C. Sator, and R. Müller, *A particle finite element method for machining simulations.* Computational Mechanics, 2014. **54**(1): p. 123-131.
121. Rodríguez, J., et al., *A Sensibility Analysis to Geometric and Cutting Conditions Using the Particle Finite Element Method (PFEM).* Procedia CIRP, 2013. **8**: p. 105-110.

122. Fraunhofer. *FPM- Finite Pointset Method.* 2016 20/02/2016]; Available from: http://www.itwm.fraunhofer.de/en/departments/transport-processes/products/fpm-finite-pointset-method.html.

123. Uhlmann, E., R. Gerstenberger, and J. Kuhnert, *Cutting Simulation with the Meshfree Finite Pointset Method.* Procedia CIRP, 2013. **8**: p. 391-396.

124. Uhlmann, E., et al. *The finite pointset method for the meshfree numerical simulation of chip formation.* 2009.

125. P.A Cundall, O.D.L.S., *A discrete numerical model for granular assemblies.* Geotechnique, 1979. **29**(1): p. 47-65.

126. Tan, Y., D. Yang, and Y. Sheng, *Study of polycrystalline Al2O3 machining cracks using discrete element method.* International Journal of Machine Tools and Manufacture, 2008. **48**(9): p. 975-982.

127. Eberhard, P. and T. Gaugele, *Simulation of cutting processes using mesh-free Lagrangian particle methods.* Computational Mechanics, 2012. **51**(3): p. 261-278.

128. Qiu, Y., M. Gu, and Z. Wei, *Machining mechanism research of glass by discrete element method.* Journal of Mechanical Science and Technology, 2015. **29**(3): p. 1283-1288.

129. Fleissner, F., T. Gaugele, and P. Eberhard, *Applications of the discrete element method in mechanical engineering.* Multibody System Dynamics, 2007. **18**(1): p. 81-94.

130. Tan, Y., D. Yang, and Y. Sheng, *Discrete element method (DEM) modeling of fracture and damage in the machining process of polycrystalline SiC.* Journal of the European Ceramic Society, 2009. **29**(6): p. 1029-1037.

131. Iliescu, D., et al., *A discrete element method for the simulation of CFRP cutting.* Composites Science and Technology, 2010. **70**(1): p. 73-80.

132. Cleary, P.W., M. Prakash, and J. Ha, *Novel applications of smoothed particle hydrodynamics (SPH) in metal forming.* Journal of Materials Processing Technology, 2006. **177**(1-3): p. 41-48.

133. Madaj, M. and M. Píška, *On the SPH Orthogonal Cutting Simulation of A2024-T351 Alloy.* Procedia CIRP, 2013. **8**: p. 152-157.

134. Rüttimann, N., et al., *Simulation of Hexa-Octahedral Diamond Grain Cutting Tests Using the SPH Method.* Procedia CIRP, 2013. **8**: p. 322-327.

135. Das, R. and P.W. Cleary, *Effect of rock shapes on brittle fracture using Smoothed Particle Hydrodynamics.* Theoretical and Applied Fracture Mechanics, 2010. **53**(1): p. 47-60.

136. Bui, H.H., et al., *Lagrangian meshfree particles method (SPH) for large deformation and failure flows of geomaterial using elastic-plastic soil constitutive model.* International Journal for Numerical and Analytical Methods in Geomechanics, 2008. **32**(12): p. 1537-1570.

137. Lin, J., et al., *Efficient meshless SPH method for the numerical modeling of thick shell structures undergoing large deformations.* International Journal of Non-Linear Mechanics, 2014. **65**: p. 1-13.

138. Nordendale, N.a., W.F. Heard, and P.K. Basu, *Modeling of High-Rate Ballistic Impact of Brittle Armors with Abaqus / Explicit.* 2012. p. 1-14.

139. Russel, K.S., *Smoothed particle hdyrodynamics modelling for failure in metals.* 2010. p. 328-328.

140. Villumsen, M.F. and T.G. Fauerholdt. *Simulation of Metal Cutting using Smooth Particle Hydrodynamics.* 2008. DYNAmore GmbH.

141. Zhao, H., et al., *Influences of sequential cuts on micro-cutting process studied by smooth particle hydrodynamic (SPH).* Applied Surface Science, 2013. **284**: p. 366-371.

142. Gąsiorek, D., *The application of the smoothed particle hydrodynamics (SPH) method and the experimental verification of cutting of sheet metal bundles using a guillotine.* Journal of Theoretical and Applied Mechanics, 2013. **51**(4): p. 1053-1065.

143. Xi, Y., et al., *SPH/FE modeling of cutting force and chip formation during thermally assisted machining of Ti6Al4V alloy.* Computational Materials Science, 2014. **84**: p. 188-197.

144. Guo, X., et al., *A numerical model for optical glass cutting based on SPH method.* The International Journal of Advanced Manufacturing Technology, 2013. **68**(5-8): p. 1277-1283.

145. Calamaz, M., et al., *Toward a better understanding of tool wear effect through a comparison between experiments and SPH numerical modelling of machining hard materials.* International Journal of Refractory Metals and Hard Materials, 2009. **27**(3): p. 595-604.

146. Lungu, N.C.S.M.B.M., *Optimization of Cutting Tool Geometrical Parameters Using Taguchi Method.* Academic Journal of Manufacturing Engineering, 2013. **11**(4): p. 62-67.

147. Makadia, A.J. and J.I. Nanavati, *Optimisation of machining parameters for turning operations based on response surface methodology.* Measurement, 2013. **46**(4): p. 1521-1529.

148. Shetty, R., et al., *Taguchi's technique in machining of metal matrix composites.* Journal of the Brazilian Society of Mechanical Sciences and Engineering, 2009. **31**(1): p. 12-20.

149. Malakizadi, A., et al., *Inverse identification of flow stress in metal cutting process using Response Surface Methodology.* Simulation Modelling Practice and Theory, 2016. **60**: p. 40-53.

150. Lin, Z.-C. and Y.-Y. Lin, *A study of an oblique cutting model.* Journal of Materials Processing Technology, 1999. **86**(1-3): p. 119-130.

151. Lin, Z.C. and Y.Y. Lin, *A study of oblique cutting for different low cutting speeds.* Journal of Materials Processing Technology, 2001. **115**(3): p. 313-325.

152. Lin, Z.-C. and Y.-Y. Lin, *Fundamental modeling for oblique cutting by thermo-elastic-plastic FEM.* International Journal of Mechanical Sciences, 1999. **41**: p. 941-965.

153. Bacaria, J.L. and O. Dalverny, *2D and 3D numerical models of metal cutting with damage effects.* Computer methods in, 2004(September): p. 11-14.

154. T.D. Marusich, M.O., *Modeling and simulation of high speed machining.* International Journal for Numerical Methods in Engineering, 1995. **38**: p. 3675-3694.

155. Ducobu, F., E. Rivière-Lorphèvre, and E. Filippi, *Numerical contribution to the comprehension of saw-toothed Ti6Al4V chip formation in orthogonal cutting.* International Journal of Mechanical Sciences, 2014. **81**: p. 77-87.

156. Zienkiewicz, O.C., R.L. Taylor, and J.Z. Zhu, *Automatic Mesh Generation*, in *The finite element method: Its basis and fundamentals.* 2013, Elsevier.

157. Barge, M., et al., *Numerical modelling of orthogonal cutting: influence of numerical parameters.* Journal of Materials Processing Technology, 2005. **164-165**: p. 1148-1153.

158. Bäker, M., *Finite element simulation of high-speed cutting forces.* Journal of Materials Processing Technology, 2006. **176**(1-3): p. 117-126.

159. Childs, T., K. Maekawa, T. Obikawa, and Y. Yamane,, *Chip formation fundamentals*, in *metal machining theory and applications*. 2000, John Wiley and Sons Ltd.

160. Han, X., *Analysis Precision Machining Process Using Finite Element Method.* 2012.

161. Zienkiewicz, C., *The finite element method in engineering science: Ch. 18.* 2nd edn. ed. 1971, London: McGraw-Hill.

162. Kakino, Y., *Analysis of the Mechanism of Orthogonal Machining by the Finite Element Method.* Journal of the Japan Society of Precision Engineering, 1971. **37**(438): p. 503-508.

163. Shirakashi, T. and E. Usui, *Simulation Analysis of Orthogonal Metal Cutting Process.* Journal of the Japan Society of Precision Engineering, 1976. **42**(496): p. 340-345.

164. Childs, T., et al., *Finite Element Methods*, in *Metal machining theory and applications.* 2000, John Wiley and Sons Ltd.

165. M.H. Dirikolu∗, T.H.C.C., K. Maekawa, *Finite element simulation of chip ow in metal machining.* International Journal of Mechanical Sciences, 2001.

166. Lin, Z.C. and W.C. Pan, *A thermoelastic-plastic large deformation model for orthogonal cutting with tool flank wear - Part 2: Machining application.* Int. J. Mech. Sci., 1993. **35**(10): p. 829-840.

167. Lin, Z.C. and S.Y. Lin, *A Coupled Finite Element Model of Thermo-Elastic-Plastic Large Deformation for Orthogonal Cutting.* Journal of Engineering Materials and Technology, 1992. **114**(2): p. 218.

168. Hillerborg, A., M. Mod´eer, and P.E. Petersson, *Analysis of crack formation and crack growth in concrete by means of fracture mechanics and finite elements.* Cement and Concrete Research, 1976. **6**: p. 773-782.

169. Hashemi, J., A.A. Tseng, and P.C. Chou, *Finite element modeling of segmental chip formation in high-speed orthogonal cutting.* Journal of Materials Engineering and Performance, 1994. **3**(6): p. 712-721.

170. Owen, D.R.J. and M. Vaz, *Computational techniques applied to high-speed machining under adiabatic strain localization conditions.* Computer Methods in Applied Mechanics and Engineering, 1999. **171**(3-4): p. 445-461.

171. Lemaitre, J., *A Continuous Damage Mechanics Model for Ductile Fracture.* J. Eng. Mater. Technol.(Trans. ASME), 1985. **107**(January 1985): p. 83-89.

172. Chen, G., et al., *Measurement and finite element simulation of micro-cutting temperatures of tool tip and workpiece.* International Journal of Machine Tools and Manufacture, 2013. **75**: p. 16-26.

173. Ducobu, F., E. Rivière-Lorphèvre, and E. Filippi, *Influence of the Material Behavior Law and Damage Value on the Results of an Orthogonal Cutting Finite Element Model of Ti6Al4V.* Procedia CIRP, 2013. **8**: p. 379-384.

174. Guerra Silva, R., et al., *Finite element modeling of chip separation in machining cellular metals.* Advances in Manufacturing, 2015. **3**(1): p. 54-62.

175. Xie, J.Q., A.E. Bayoumi, and H.M. Zbib, *FEA modeling and simulation of shear localized chip formation in metal cutting.* International Journal of Machine Tools and Manufacture, 1998. **38**(9): p. 1067-1087.

176. Xlet, J.Q.B.A.E.Z.H.M., *A study on shear banding in chip formation of orthogonal machining.* International Journal of Machine Tools and Manufacture, 1996. **36**(7): p. 835-847.

177. Guo, J.Y. and M. Lv, *Explicit Finite Element Simulation of Oblique Cutting Process.* Key Engineering Materials, 2010. **431-432**: p. 297-300.
178. Iwata, K., K. Osakada, and Y. Terasaka, *Process Modeling of Orthogonal Cutting by the Rigid-Plastic Finite Element Method.* Journal of Engineering Materials and Technology, 1984. **106**(2): p. 132.
179. Obikawa, T., et al., *Application of Computational Machining Method to Discontinuous Chip Formation.* Journal of Manufacturing Science and Engineering, 1997. **119**(4B): p. 667-667.
180. Zhang, B. and A. Bagchi, *Finite Element Simulation of Chip Formation and Comparison with Machining Experiment.* Journal of Engineering for Industry, 1994. **116**(3): p. 289.
181. Ueda, K. and K. Manabe, *Rigid-Plastic FEM Analysis of Three-Dimensional Deformation Field in Chip Formation Process.* CIRP Annals - Manufacturing Technology, 1993. **42**(1): p. 35-38.
182. Huang, J.M. and J.T. Black, *An Evaluation of Chip Separation Criteria for the FEM Simulation of Machining.* Journal of Manufacturing Science and Engineering, 1996. **118**(4): p. 545.
183. Chandrakanth Shet, X.D., *Finite element analysis of the orthogonal metal cutting process.* Journal of Materials Processing Technology, 2000. **105**(April 1999): p. 95-109.
184. Guoqin, S., D. Xiaomin, and C. Shet, *A finite element study of the effect of friction in orthogonal metal cutting.* Finite Elements in Analysis and Design, 2002. **38**(9): p. 863-883.
185. Gordon R. Johnson, W.H.C., *Fracture characteristics of three metals subjected to various strains, strain rate, temperatures and pressures.* Engineering Fracture Mechanics, 1985. **21**(1): p. 31-48.
186. Mabrouki, T., et al., *Numerical and experimental study of dry cutting for an aeronautic aluminium alloy (A2024-T351).* International Journal of Machine Tools and Manufacture, 2008. **48**(11): p. 1187-1197.
187. Hortig, C. and B. Svendsen, *Simulation of chip formation during high-speed cutting.* Journal of Materials Processing Technology, 2007. **186**(1-3): p. 66-76.
188. Atul A.a Jadhav, M.S.R., *Finite Element Simulation of Orthogonal Cutting Process for Steel.* International Journal of Engineering Research & Technology, 2015. **4**(4).
189. Elwasli, F., et al., *A 3D multi-scratch test model for characterizing material removal regimes in 5083-Al alloy.* Materials & Design, 2015. **87**: p. 352-362.
190. Ng, E.-G., et al., *Physics-Based Simulation of High Speed Machining.* Machining Science and Technology, 2002. **6**(3): p. 301-329.
191. T.T.Öpöz, X.C., *Ffinite element simulation of chip formation*, in *School of Computing and Engineering Researchers' Conference*. 2010, University of Huddersfield: Huddersfield. p. 166-171.
192. Subbiah, S., et al., *Evidence of Ductile Tearing Ahead of the Cutting Tool and Modeling the Energy Consumed in Material Separation in Micro-Cutting.* 2006. **2006**: p. 499-508.
193. Ceretti, E., M. Lucchi, and T. Altan, *FEM simulation of orthogonal cutting: serrated chip formation.* Journal of Materials Processing Technology, 1999. **95**(1-3): p. 17-26.
194. Wang, B. and Z. Liu, *Shear localization sensitivity analysis for Johnson–Cook constitutive parameters on serrated chips in high speed machining of Ti6Al4V.* Simulation Modelling Practice and Theory, 2015. **55**: p. 63-76.

195. Lee, H.C., et al., *Application of element deletion method for numerical analyses of cracking.* Manufacturing Engineering, 2009. **35**(2): p. 154-161.
196. Simulia, D., *Abaqus 6.14 documentation.* 2014.
197. Vaziri, M.R., M. Salimi, and M. Mashayekhi, *Evaluation of chip formation simulation models for material separation in the presence of damage models.* Simulation Modelling Practice and Theory, 2011. **19**(2): p. 718-733.
198. Sawarkar, N., *Finite Element based Simulation of Orthogonal Cutting Process to Determine Residual Stress Induced.* International journal of computer applications, 2014: p. 33-38.
199. Schulze, V. and F. Zanger, *Development of a Simulation Model to Investigate Tool Wear in Ti-6Al-4V Alloy Machining.* Advanced Materials Research, 2011. **223**: p. 535-544.
200. Mamalis, A.G., A.S. Branis, and D.E. Manolakos, *Modelling of precision hard cutting using implicit finite element methods.* Journal of Materials Processing Technology, 2002. **123**(3): p. 464-475.
201. Ee, K.C., O.W. Dillon, and I.S. Jawahir, *Finite element modeling of residual stresses in machining induced by cutting using a tool with finite edge radius.* International Journal of Mechanical Sciences, 2005. **47**(10): p. 1611-1628.
202. Zong, W.J., et al., *Finite element optimization of diamond tool geometry and cutting-process parameters based on surface residual stresses.* The International Journal of Advanced Manufacturing Technology, 2006. **32**(7-8): p. 666-674.
203. Branco, R., F.V. Antunes, and J.D. Costa, *A review on 3D-FE adaptive remeshing techniques for crack growth modelling.* Engineering Fracture Mechanics, 2015. **141**: p. 170-195.
204. Lei, S., Y.C. Shin, and F.P. Incropera, *Thermo-mechanical modeling of orthogonal machining process by finite element analysis.* International Journal of Machine Tools and Manufacture, 1999. **39**: p. 731-750.
205. Hua, J. and R. Shivpuri, *Prediction of chip morphology and segmentation during the machining of titanium alloys.* Journal of Materials Processing Technology, 2004. **150**(1-2): p. 124-133.
206. Childs, T., K. Maekawa, T. Obikawa, and Y. Yamane,, *Application of finite element analysis*, in *Metal machining theory and applications.* 2000, John Wiley and Sons Ltd.
207. Shivpuri, R., et al., *Microstructure-Mechanics Interactions in Modeling Chip Segmentation during Titanium Machining.* CIRP Annals - Manufacturing Technology, 2002. **51**(1): p. 71-74.
208. Zhang, X.P., R. Shivpuri, and A.K. Srivastava, *Role of phase transformation in chip segmentation during high speed machining of dual phase titanium alloys.* Journal of Materials Processing Technology, 2014. **214**(12): p. 3048-3066.
209. Bäker, M., J. Rösler, and C. Siemers, *The Influence of Thermal Conductivity on Segmented Chip formation.* Computational Materials Science, 2003. **26**: p. 175-182.
210. Obikawa, T. and E. Usui, *Computational Machining of Titanium Alloy—Finite Element Modeling and a Few Results.* Journal of Manufacturing Science and Engineering, 1996. **118**(2): p. 208.
211. Zhang, Y., et al., *Cutting simulation capabilities based on crystal plasticity theory and discrete cohesive elements.* Journal of Materials Processing Technology, 2012. **212**(4): p. 936-953.

212. Vaziri, M.R., M. Salimi, and M. Mashayekhi, *A new calibration method for ductile fracture models as chip separation criteria in machining.* Simulation Modelling Practice and Theory, 2010. **18**(9): p. 1286-1296.

213. Guo, Y.B., Q. Wen, and K.A. Woodbury, *Dynamic Material Behavior Modeling Using Internal State Variable Plasticity and Its Application in Hard Machining Simulations.* Journal of Manufacturing Science and Engineering, 2006. **128**(3): p. 749.

214. Guo, Y.B. and D.W. Yen, *A FEM study on mechanisms of discontinuous chip formation in hard machining.* Journal of Materials Processing Technology, 2004. **155-156**: p. 1350-1356.

215. Calamaz, M., D. Coupard, and F. Girot, *A new material model for 2D numerical simulation of serrated chip formation when machining titanium alloy Ti–6Al–4V.* International Journal of Machine Tools and Manufacture, 2008. **48**(3-4): p. 275-288.

216. Rhim, S.-H. and S.-I. Oh, *Prediction of serrated chip formation in metal cutting process with new flow stress model for AISI 1045 steel.* Journal of Materials Processing Technology, 2006. **171**(3): p. 417-422.

217. Umbrello, D., *Finite element simulation of conventional and high speed machining of Ti6Al4V alloy.* Journal of Materials Processing Technology, 2008. **196**(1-3): p. 79-87.

218. Aurich, J.C. and H. Bil, *3D Finite Element Modelling of Segmented Chip Formation.* CIRP Annals - Manufacturing Technology, 2006. **55**(1): p. 47-50.

219. Deng, W.J., et al., *Finite Element Modelling and Simulation of Chip Breaking with Grooved Tool.* International Journal of Simulation Modelling, 2013. **12**(4): p. 264-275.

220. Liu, J., Y. Bai, and C. Xu, *Evaluation of Ductile Fracture Models in Finite Element Simulation of Metal Cutting Processes.* Journal of Manufacturing Science and Engineering, 2013. **136**(1): p. 011010.

221. Ueda, K., T. Sugita, and H. Tsuwa, *Application of Fracture Mechanics in Micro-Cutting of Engineering Ceramics.* CIRP ANNALS-MANUFACTURING TECHNOLOGY, 1983. **32**: p. 83-86.

222. Ueda, K., et al., *A J-Integral Approach to Material Removal Mechanisms in Microcutting of Ceramics.* CIRP Annals - Manufacturing Technology, 1991. **40**(1): p. 61-64.

223. Bailey, J.A., *Friction in Mechanical Machining -- Mechanical Aspects.* Wear, 1975. **31**: p. 243-275.

224. Durul Ulutan, T.Ö., *Methodology to determine friction in orthogonal cutting with application to machiningi titanium and nickle based alloys*, in *International Manufacturing Science and Engineering Conference.* 2012, Proceedings of the ASME 2012: Notre Dame, Indiana , USA.

225. Oraby, S.E. and A.M. Alaskari, *Mathematical Modeling Experimental Approach of the Friction on the Tool-Chip Interface of Multicoated Carbide Turning Inserts.* International journal of mechanical, aerospace, industrial, mechatronic and manufacturing engineering, 2011. **5**(3): p. 455-465.

226. Abouridouane, M., et al., *The Mechanics of Cutting: In-situ Measurement and Modelling.* Procedia CIRP, 2015. **31**: p. 246-251.

227. Filice, L., et al., *A critical analysis on the friction modelling in orthogonal machining.* International Journal of Machine Tools and Manufacture, 2007. **47**(3-4): p. 709-714.

228. Özel, T. and E. Zeren, *Determination of work material flow stress and friction for FEA of machining using orthogonal cutting tests.* Journal of Materials Processing Technology, 2004. **153-154**: p. 1019-1025.

229. Barrow, G., et al., *Determination of rake face stress distribution in orthogonal machining.* International Journal of Machine Tool Design and Research, 1982. **22**(1): p. 75-85.

230. Buryta, D., R. Sowerby, and I. Yellowley, *Stress distribution on the rake face during orthogonal machining.* International Journal of Machine Tools and Manufacture, 1994. **34**(5): p. 721-739.

231. Issa, M., et al., *Numerical prediction of thermomechanical field localization in orthogonal cutting.* CIRP Journal of Manufacturing Science and Technology, 2012. **5**(3): p. 175-195.

232. Kara, F., K. Aslantaş, and A. Çiçek, *Prediction of cutting temperature in orthogonal machining of AISI 316L using artificial neural network.* Applied Soft Computing, 2016. **38**: p. 64-74.

233. Usui E., S.T., *Mechanics of machining—from descriptive to predictive theory. In: On the art of cutting metals—75 years later.* ASME Publication PED, 1982. **7**: p. 13-35.

234. Zorev, N.N. *Interrelationship between shear processes occurring along tool face and on shear plane in metal cutting.* 1963.

235. Ozel, T. and T. Altan, *Determination of workpiece flow stress and friction at the chip-tool contact for high-speed cutting.* International Journal of Machine Tools and Manufacture, 2000. **40**(1): p. 133-152.

236. Buchkremer, S., F. Klocke, and D. Lung, *Finite-element-analysis of the relationship between chip geometry and stress triaxiality distribution in the chip breakage location of metal cutting operations.* Simulation Modelling Practice and Theory, 2015. **55**: p. 10-26.

237. Li, X., *Development of a predictive model for stress distributions at the tool-chip interface in machining.* Journal of materials processing technology, 1997. **0136**(96).

238. Kim, K.W. and H.-C. Sins, *Development of a thermo-viscoplastic cutting model using finite element method.* International Journal of Machine Tools and Manufacture, 1996. **36**(3): p. 379-397.

239. Childs, T.H.C. and K. Maekawa, *Computer-Aided Simulation and Experimental Studies of Chip Flow and Tool Wear in the Turning of Low-Alloy Steels by Cemented Carbide Tools.* Wear, 1990. **139**(2): p. 235-250.

240. Egaña, A., J. Rech, and P.J. Arrazola, *Characterization of Friction and Heat Partition Coefficients during Machining of a TiAl6V4 Titanium Alloy and a Cemented Carbide.* Tribology Transactions, 2012. **55**(5): p. 665-676.

241. Zemzemi, F., et al., *Identification of a friction model at tool/chip/workpiece interfaces in dry machining of AISI4142 treated steels.* Journal of Materials Processing Technology, 2009. **209**(8): p. 3978-3990.

242. Brocail, J., et al., *Contact and friction analysis at tool-chip interface to high-speed machining.* International Journal of Material Forming, 2008. **1**(S1): p. 1407-1410.

243. Mishra, R.k., Goel S, Yazdani Nezhad H., *Computational Prediction of electrical and thermal properties of graphene and BaTiO3 reinforced epoxy nanocomposites. Biomaterial and Polymers Horizons.* Biomaterials and Polymers Horizons, 2021. **1**: p. 1-14.

244. Sasahara, H., T. Obikawa, and T. Shirakashi, *FEM analysis of cutting sequence effect on mechanical characteristics in machined layer.* Journal of Materials Processing Technology, 1996. **62**(4): p. 448-453.

245. Bawaneh, M.A. and V. Madhavan, *Determination of Material Constitutive Models using Orthogonal Machining Tests.* Department of Industrial and Manufacturing Engineering, 2007. **PhD**(December).

246. Zhang, Y., J.C. Outeiro, and T. Mabrouki, *On the Selection of Johnson-cook Constitutive Model Parameters for Ti-6Al-4V Using Three Types of Numerical Models of Orthogonal Cutting.* Procedia CIRP, 2015. **31**: p. 112-117.

247. Schulze, V. and F. Zanger, *Numerical Analysis of the Influence of Johnson-Cook-Material Parameters on the Surface Integrity of Ti-6Al-4V.* Procedia Engineering, 2011. **19**: p. 306-311.

248. Banerjee, A., et al., *An Experimental Determination of Johnson Cook Material and Failure Model Constants for Armour Steel.* Applied Mechanics and Materials, 2014. **592-594**: p. 990-995.

249. Ozel, T. and Y. Karpat, *Identification of constitutive material model parameters for high-strain rate metal cutting conditions using evolutionary computational algorithms.* Materials and Manufacturing Processes, 2007. **22**(5-6): p. 659-667.

250. BATRA, R.C. and C.H. KIM, *Effects of viscoplastic flow rules on the initiation and growth of shear bands at high strain rates.* J. Mech. Phys. Solids, 1990. **38**: p. 859-874.

251. Batra, R.C. and N.A. Jaber, *Failure mode transition speeds in an impact loaded prenotched plate with four thermoviscoplastic relations.* International Journal of Fracture, 2001. **110**(1): p. 47-71.

252. Zhan, H., et al., *Constitutive modelling of the flow behaviour of a β titanium alloy at high strain rates and elevated temperatures using the Johnson–Cook and modified Zerilli–Armstrong models.* Materials Science and Engineering: A, 2014. **612**: p. 71-79.

253. Wang, X., et al., *Dynamic behavior and a modified Johnson–Cook constitutive model of Inconel 718 at high strain rate and elevated temperature.* Materials Science and Engineering: A, 2013. **580**: p. 385-390.

254. Sartkulvanich, P., F. Koppka, and T. Altan, *Determination of flow stress for metal cutting simulation—a progress report.* Journal of Materials Processing Technology, 2004. **146**(1): p. 61-71.

255. Amiri, S., et al., *Determining Elastic-Plastic Properties of Al6061-T6 from Micro-Indentation Technique.* Key Engineering Materials, 2013. **592-593**: p. 610-613.

256. E. Usui, T.S. and T. Kitagawa, *Analytical prediction of cutting tool wear.* Wear, 1984. **100**: p. 129-151.

257. Dan, L. and J. Mathew, *Tool wear and failure monitoring techniques for turning-A review.* International Journal of Machine Tools and Manufacture, 1990. **30**(4): p. 579-598.

258. Takeyama, H. and R. Murata, *Basic Investigation of Tool Wear.* Journal of Engineering for Industry, 1963. **85**(1): p. 33.

259. Shimada, S., et al., *Thermo-Chemical Wear Mechanism of Diamond Tool in Machining of Ferrous Metals.* CIRP Annals - Manufacturing Technology, 2004. **53**(1): p. 57-60.

260. Matsumura, T., et al., *Autonomous turning operation planning with adaptive prediction of tool wear and surface roughness.* Journal of Manufacturing Systems, 1993. **12**(3): p. 253-262.

261. Attanasio, A., E. Ceretti, and C. Giardini, *Analytical Models for Tool Wear Prediction During AISI 1045 Turning Operations.* Procedia CIRP, 2013. **8**: p. 218-223.

262. Taylor, J., *The tool wear-time relationship in metal cutting.* International Journal of Machine Tool Design and Research, 1962. **2**(2): p. 119-152.

263. Dos Santos, A.L.B., et al., *An optimisation procedure to determine the coefficients of the extended Taylor's equation in machining.* International Journal of Machine Tools & Manufacture, 1999. **39**(1): p. 17-31.

264. Ojha, D.K. and U.S. Dixit, *An economic and reliable tool life estimation procedure for turning.* The International Journal of Advanced Manufacturing Technology, 2005. **26**(7-8): p. 726-732.

265. Binder, M., F. Klocke, and D. Lung, *Tool wear simulation of complex shaped coated cutting tools.* Wear, 2015. **330-331**: p. 600-607.

266. List, G., G. Sutter, and A. Bouthiche, *Cutting temperature prediction in high speed machining by numerical modelling of chip formation and its dependence with crater wear.* International Journal of Machine Tools and Manufacture, 2012. **54-55**: p. 1-9.

267. Molinari, A. and M. Nouari, *Modeling of tool wear by diffusion in metal cutting.* Wear, 2002. **252**(1-2): p. 135-149.

268. Filice, L., et al., *Wear modelling in mild steel orthogonal cutting when using uncoated carbide tools.* Wear, 2007. **262**(5-6): p. 545-554.

269. Zanger, F. and V. Schulze, *Investigations on Mechanisms of Tool Wear in Machining of Ti-6Al-4V Using FEM Simulation.* Procedia CIRP, 2013. **8**: p. 158-163.

270. MacGinley, T. and J. Monaghan, *Modelling the Orthogonal Machining Process Using Cutting Tools With Different Geometry.* Journal of Materials Processing Technology, 2001. **118**: p. 293-300.

271. Matsumura, T., T. Shirakashi, and E. Usui, *Identification of Wear Characteristics in Tool Wear Model of Cutting Process.* International Journal of Material Forming, 2008. **1**(S1): p. 555-558.

272. Yen, Y.C., et al., *Estimation of Tool Wear of Carbide Tool in Orthogonal Cutting Using Fem Simulation.* Machining Science and Technology, 2002. **6**(3): p. 467-486.

273. Ceretti, E., et al., *Diffusion wear modelling in 3D cutting process.* International journal of machining and machinability of materials, 2009. **6**(1/2): p. 10-12.

274. Mathew, P., *Use of predicted cutting temperatures in determining tool performance.* International Journal of Machine Tools and Manufacture, 1989. **29**(4): p. 481-497.

275. Lorentzon, J. and N. Järvstråt, *Modelling tool wear in cemented-carbide machining alloy 718.* International Journal of Machine Tools and Manufacture, 2008. **48**(10): p. 1072-1080.

276. Salvatore, F., S. Saad, and H. Hamdi, *Modeling and Simulation of Tool Wear During the Cutting Process.* Procedia CIRP, 2013. **8**: p. 305-310.

277. Yue, C.X., et al., *2D FEM Estimate of Tool Wear in Hard Cutting Operation: Extractive of Interrelated Parameters and Tool Wear Simulation Result.* Advanced Materials Research, 2009. **69-70**: p. 316-321.

278. Li, K., X.L. Gao, and J.W. Sutherland, *Finite element simulation of the orthogonal metal cutting process for qualitative understanding of the effects of crater wear on the chip formation process.* Journal of Materials Processing Technology, 2002. **127**(3): p. 309-324.

279. Ducobu, F., et al., *Finite Element Prediction of the Tool Wear Influence in Ti6Al4V Machining.* Procedia CIRP, 2015. **31**: p. 124-129.

280. Lo, S.P., *An analysis of cutting under different rake angles using the finite element method.* Journal of Materials Processing Technology, 2000. **105**(1-2): p. 143-151.

281. Shi, J. and C.R. Liu, *The Influence of Material Models on Finite Element Simulation of Machining.* Journal of Manufacturing Science and Engineering, 2004. **126**(4): p. 849.

282. Lei, S., Y.C. Shin, and F.P. Incropera, *Material constitutive modeling under high strain rates and temperatures through orthogonal machining tests.* Journal of Manufacturing Science and Engineering, Transactions of the ASME, 1999. **121**(4): p. 577-585.

283. Jaspers, S.P.F.C. and J.H. Dautzenberg, *Material behaviour in metal cutting: strains, strain rates and temperatures in chip formation.* Journal of Materials Processing Technology, 2002. **121**(1): p. 123-135.

284. Abukhshim, N.A., P.T. Mativenga, and M.A. Sheikh, *Heat generation and temperature prediction in metal cutting: A review and implications for high speed machining.* International Journal of Machine Tools and Manufacture, 2006. **46**(7-8): p. 782-800.

285. Kore Mahesh, J.T.P., SN Joshi, Basil Kuriachen, *Machinability of Inconel 718: A critical review on the impact of cutting temperatures.* Materials and Manufacturing Processes, 2021. **36**(7): p. 753-791.

286. Maekawa, K., Y. Nakano, and T. Kitagawa, *Finite element analysis of thermal behaviour in metal machining (Ist report, influence of thermophysical properties on cutting temperature).* Transactions of Japenese society of mechanical engineers, 1996. **62**(596): p. 1587-1593.

287. Tay, A.O., M.G. Stevenson, and G.d.V. Davis, *Using the finite element method to determine temperature distributions in orthogonal machining.* ARCHIVE: Proceedings of the Institution of Mechanical Engineers 1847-1982 (vols 1-196), 1974. **188**(1974): p. 627-638.

288. Analysis, S. and I. Saulcy, *Residual stresses in orthogonal cutting of metals: The effect of thermomechanical coupling parameter and of friction.* Journal of thermal stresses, 2009. **32**(3): p. 269-289.

289. Shrikrishna Nandkishor Joshi, G.B., *Three-dimensional finite element based numerical simulation of machining of thin-wall components with varying wall constraints.* Journal of The Institution of Engineers (India): Series C, 2017. **98**(3): p. 343-352.

290. Childs, T.H.C., M.I. Mahdi, and G. Barrow, *On the Stress Distribution Between the Chip and Tool During Metal Turning.* CIRP Annals - Manufacturing Technology, 1989. **38**(1): p. 55-58.

291. Oxley, P.L.B. and A.P. Hatton, *shear angle solution based on experimental shear zone and tool chip interface stress distribution.* International Journal of Mechanical Sciences, 1963. **5**: p. 41-55.

292. T. TYAN , W.H.Y., *Analysis of orthogonal metal cutting processes.* International Journal for Numerical Methods in Engineering, 1992. **34**: p. 365-389.

293. Guo, Y.B., *Finite element modeling of residual stress profile patterns in hard turning.* JCPDS-International centre for diffraction data, 2009. **24**: p. 344-351.
294. Liu, M., J.-i. Takagi, and A. Tsukuda, *Effect of tool nose radius and tool wear on residual stress distribution in hard turning of bearing steel.* Journal of Materials Processing Technology, 2004. **150**(3): p. 234-241.
295. Dahlman, P., F. Gunnberg, and M. Jacobson, *The influence of rake angle, cutting feed and cutting depth on residual stresses in hard turning.* Journal of Materials Processing Technology, 2004. **147**(2): p. 181-184.
296. Outeiro, J.C., D. Umbrello, and R. M'Saoubi, *Experimental and numerical modelling of the residual stresses induced in orthogonal cutting of AISI 316L steel.* International Journal of Machine Tools and Manufacture, 2006. **46**(14): p. 1786-1794.
297. Wu, D.W. and Y. Matsumoto, *The Effect of Hardness on Residual Stresses in Orthogonal Machining of AISI 4340 Steel.* Journal of Engineering for Industry, 1990. **112**(3): p. 245.
298. Outeiro, J.C., et al., *Analysis of residual stresses induced by dry turning of difficult-to-machine materials.* CIRP Annals - Manufacturing Technology, 2008. **57**(1): p. 77-80.
299. Yang, X. and C.R. Liu, *A new stress-based model of friction behavior in machining and its significant impact on residual stresses computed by finite element method.* International Journal of Mechanical Sciences, 2002. **44**(4): p. 703-723.
300. Liu, C.R. and Y.B. Guo, *Finite element analysis of the effect of sequential cuts and tool chip friction on residual stresses in a machined layer.* International Journal of Mechanical Sciences, 2000. **42**: p. 1069-1086.
301. Liu, C.R. and M.M. Barash, *The Mechanical State of the Sublayer of a Surface Generated by Chip-Removal Process—Part 2: Cutting With a Tool With Flank Wear.* Journal of Engineering for Industry, 1976. **98**(4): p. 1202.
302. Liu, C.R. and M.M. Barash, *Variables Governing Patterns of Mechanical Residual Stress in a Machined Surface.* Journal of Engineering for Industry, 1982. **104**(3): p. 257.
303. Liu, C.R. and M.M. Barash, *The Mechanical State of the Sublayer of a Surface Generated by Chip-Removal Process—Part 1: Cutting With a Sharp Tool.* Journal of Engineering for Industry, 1976. **98**(4): p. 1192.
304. Anurag, S., Y.B. Guo, and Z.Q. Liu, *A new fem approach to predict residual stress profiles in hard turning without simulating chip formation.* Transactions of NAMRI/SME, 2010. **38**: p. 33-40.